Central exclusive production at high energies

Antoni Szczurek

INSTITUTE OF NUCLEAR PHYSICS

POLISH ACADEMY OF SCIENCES

IFJ PAN

AND

UNIVERSITY OF RZESZOW

Introduction

Exclusive reaction: $pp \to pXp$ ($X = \eta', \eta_c, \eta_b, \chi_c, \chi_b$).
At high energy - one of many open channels (!)
$\to$ rapidity gaps.

- (a) Search for Higgs primary task for LHC. Diffractive production of the Higgs an alternative to inclusive production (background reduction). A new QCD mechanism proposed recently by Khoze-Martin-Ryskin. Not possible to measure Higgs at present. Replace Higgs by a meson (scalar, pseudoscalar)
- (b) The mechanism of the exclusive production of mesons at high energy is not well known in detail.
- (c) Possibility to study differential distributions.

Our recent works

Recently we have calculated differential cross sections in:

- $pp \to pp\eta'$ ($pp \to pp\eta_c$)
- $pp \to pp\chi_c(0)$ (IP IP + $\gamma\gamma$)
- $pp \to pp\chi_c(1)$ (IP IP)
- $pp \to ppf_0(1500)$ (IP IP + $\pi^+\pi^-$)
- $pp \to ppJ/\psi$ (IP γ + γ IP)
- $pp \to pp\Upsilon$ (IP γ + γ IP)
- $pp \to pp\pi^+\pi^-$ ((IP + IR) $\otimes$ (IP + IR))
- $AA \to AA\rho^0\rho^0$ ($\gamma\gamma$)
- $pp \to ppZ^0$ (IP γ + γ IP)
- $pp \to pp\pi^0$ (Deck mechanism)

In collaboration with ...

based on:

- A. Szczurek, R. Pasechnik and O. Teryaev, hep-ph/0608302, Phys. Rev. **D75**, 054021 (2007)
- W. Schäfer and A. Szczurek, Arxiv:0705.2887, Phys. Rev. **D76**, 094014 (2007)
- R. Pasechnik, A. Szczurek and O. Teryaev, Arxiv:0709.0857, Phys. Rev. **D78** (2008)
- A. Rybarska, W. Schäfer and A. Szczurek, Arxiv:0805.0717, Phys. Lett. **B668** (2008) 126
- A. Szczurek and P. Lebiedowicz, Arxiv:0806.4896.

pre-QCD mechanism

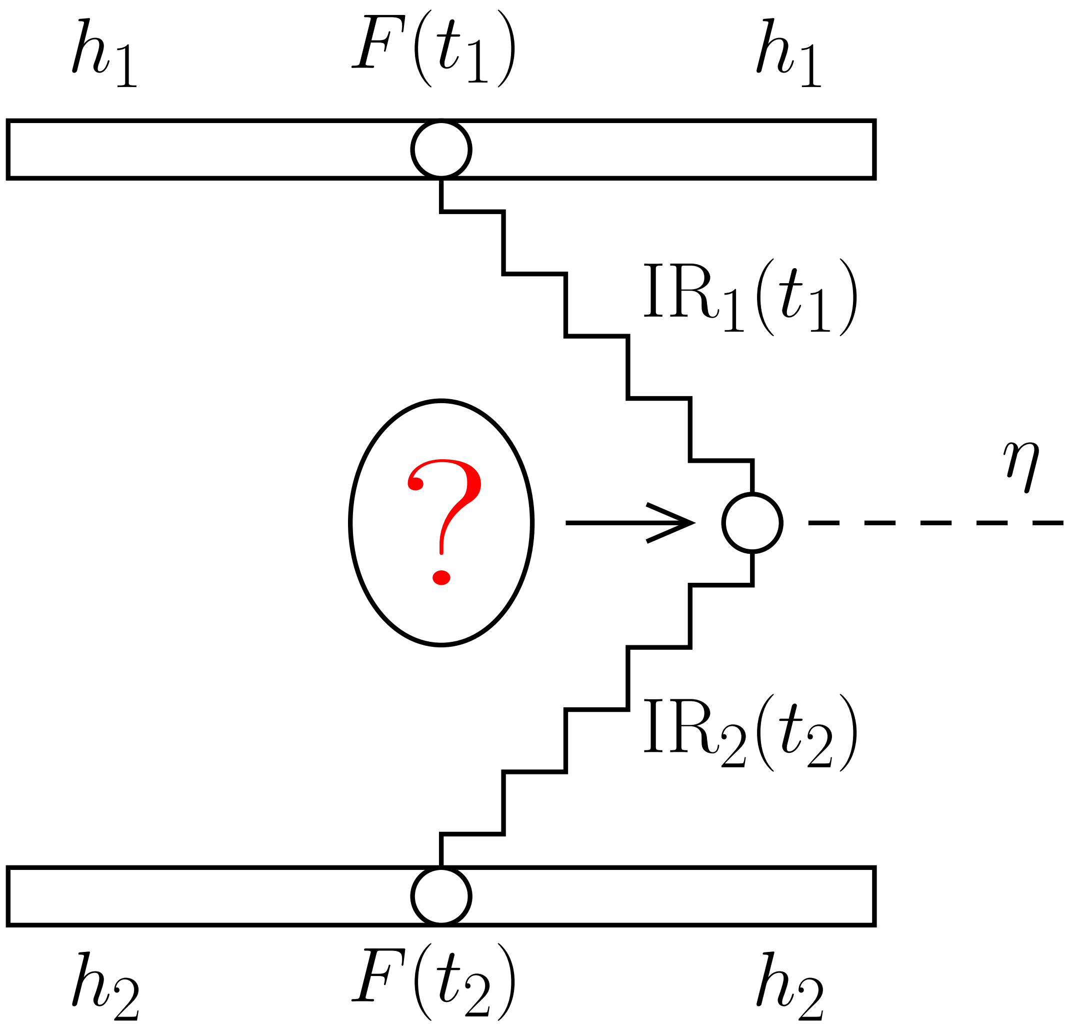

QCD motivation

HERA $\gamma^* p$ total cross section ($F_2(x, Q^2)$)

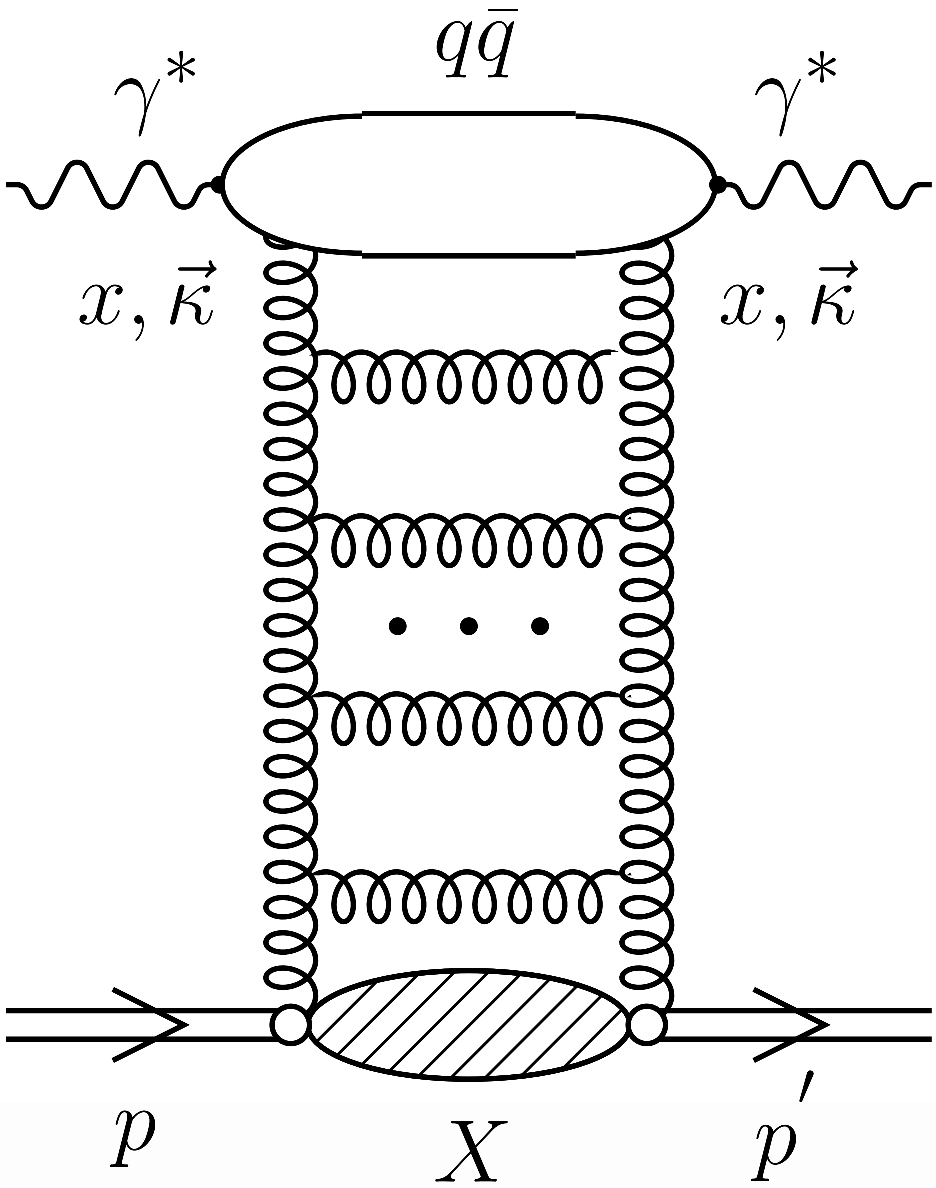

QCD mechanism

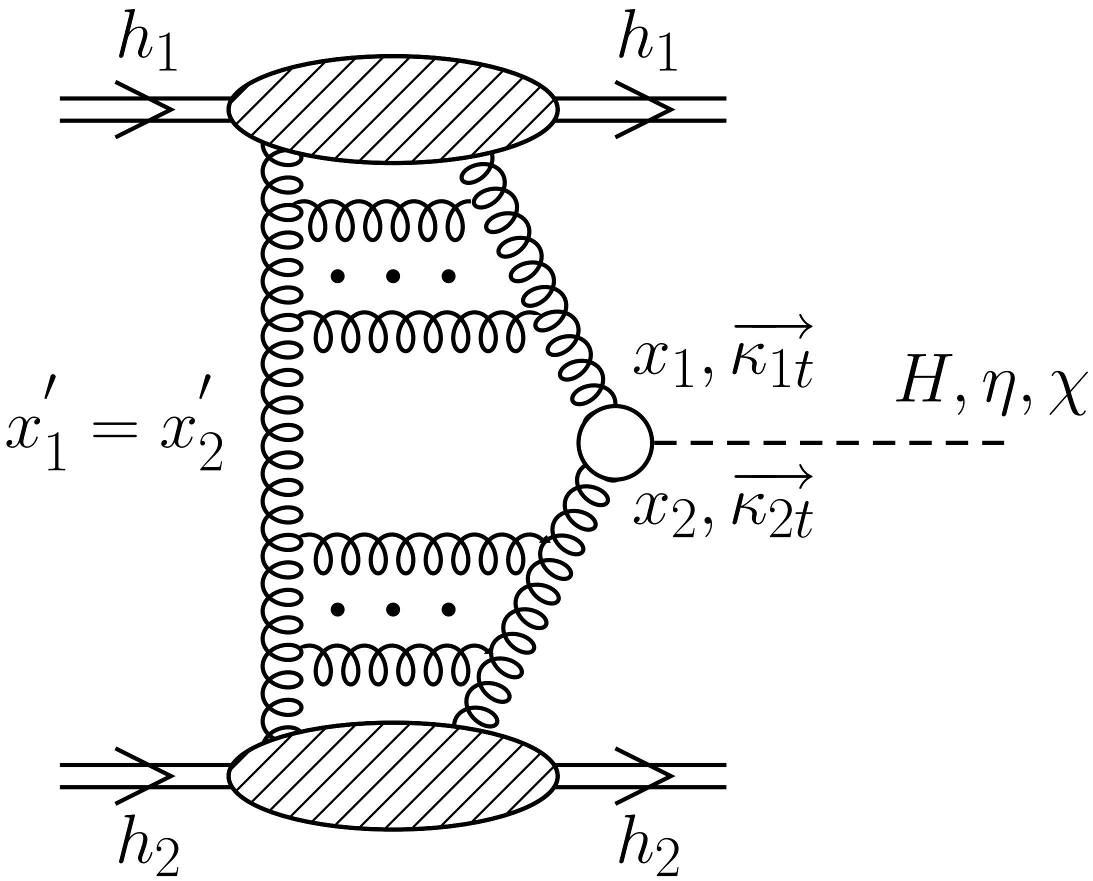

Exclusive χ_C production in proton-proton and proton-antiproton collisions

R. Pasechnik, O. Teryaev and A.S.

QCD mechanism

Khoze-Martin-Ryskin (Higgs production) (H $\to \chi_c(0)$)

$$\mathcal{M}_{pp\to p\chi_c(0)p}^{g^*g^*\to\chi_c(0)} = i\,\pi^2\, s \int d^2k_{0,t} \quad V(k_1,k_2,P_M) \tag{1}$$

$$\frac{f_g^{off}(x_1,x_1',k_{0,t}^2,k_{1,t}^2,t_1) \quad f_g^{off}(x_2,x_2',k_{0,t}^2,k_{2,t}^2,t_2)}{k_{0,t}^2\, k_{1,t}^2\, k_{2,t}^2} \,. \tag{2}$$

$f_g^{off}(...)$ – off-diagonal gluon unintegrated distributions

Off-diagonal unintegrated gluon distributions – ?

$$f_g^{off}(x_1,x_1',k_{0,t}^2,k_{1,t}^2,t_1) = \sqrt{f_g^{(1)}(x_1',k_{0,t}^2)\cdot f_g^{(1)}(x_1,k_{1,t}^2)} \cdot F_1(t_1) \tag{3}$$

$$f_g^{off}(x_2,x_2',k_{0,t}^2,k_{2,t}^2,t_2) = \sqrt{f_g^{(2)}(x_2',k_{0,t}^2)\cdot f_g^{(2)}(x_2,k_{2,t}^2)} \cdot F_1(t_2) \tag{4}$$

QCD formalism

$$\mathcal{M}^{g^* g^*} = \frac{s}{2} \cdot \pi^2 \frac{1}{2} \frac{\delta_{c_1 c_2}}{N_c^2 - 1} \int d^2 q_{0,t} V_J^{c_1 c_2}$$

$$\frac{f_{g,1}^{off}(x_1, x_1', q_{0,t}^2, q_{1,t}^2, t_1) f_{g,2}^{off}(x_2, x_2', q_{0,t}^2, q_{2,t}^2, t_2)}{q_{0,t}^2 \, q_{1,t}^2 \, q_{2,t}^2} . \quad (5)$$

$$V_J^{c_1 c_2} = \mathcal{P}(q\bar{q} \to \chi_{cJ}) \bullet \Psi_{ik}^{c_1 c_2}(k_1, k_2) \; , \quad (6)$$

$$V_{J,\,\mu\nu}^{c_1 c_2}(q_1, q_2) = \mathcal{P}(q\bar{q} \to \chi_{cJ}) \bullet \Psi_{ik,\,\mu\nu}^{c_1 c_2}(k_1, k_2) =$$

$$2\pi \cdot \sum_{i,k} \sum_{L_z, S_z} \frac{1}{\sqrt{m}} \int \frac{d^4 q}{(2\pi)^4} \delta\left(q^0 - \frac{\mathbf{q}^2}{M} \right) \times \quad (7)$$

$$\times \, \Phi_{L=1, L_z}(\mathbf{q}) \cdot \langle L = 1, L_z; S = 1, S_z | J, J_z \rangle \, \langle 3i, \bar{3}k | 1 \rangle \quad (8)$$

$$\mathrm{Tr}\left\{ \Psi_{ik,\,\mu\nu}^{c_1 c_2} \mathcal{P}_{S=1, S_z} \right\} , \quad (9)$$

$$\Psi_{ik,\,\mu\nu}^{c_1 c_2} = -g^2 \left[t_{ij}^{c_1} t_{jk}^{c_2} \cdot \left\{ \gamma_\nu \frac{\hat{q}_1 - \hat{k}_1 - m}{(q_1 - k_1)^2 - m^2} \gamma_\mu \right\} - t_{kj}^{c_2} t_{ji}^{c_1} \cdot \left\{ \gamma_\mu \frac{\hat{q}_1 - \hat{k}_2 + m}{(q_1 - k_2)^2 - m^2} \gamma_\nu \right\} \right] .$$

QCD formalism

$$\mathcal{P}_{S=1,S_z} = \frac{1}{2m}(\hat{k}_2 - m)\frac{\hat{\epsilon}(S_z)}{\sqrt{2}}(\hat{k}_1 + m) \; . \qquad (10)$$

$$\begin{aligned} \mathrm{Tr}(\Psi\, \mathcal{P}_{S=1,S_z}) \;&=\; -\delta^{c_1 c_2}\frac{\epsilon^{\rho}(S_z)}{\sqrt{2N_c}}\frac{g^2}{4m}\,\mathrm{Tr}\Bigg\{\Bigg(\gamma_\nu\frac{\hat{q}_1 - \hat{k}_1 - m}{(q_1-k_1)^2 - m^2}\gamma_\mu - \gamma_\mu\frac{\hat{q}_1 - \hat{k}_2 + m}{(q_1-k_2)^2 - m^2}\gamma_\nu\Bigg) \times \\ &\times\; (\hat{k}_2 - m)\gamma_\rho(\hat{k}_1 + m)\Bigg\}. \qquad (11 \end{aligned}$$

$$\int\frac{d^3\mathbf{q}}{(2\pi)^3}q^\sigma\Phi_{L=1,L_z}(\mathbf{q}) = -i\sqrt{\frac{3}{4\pi}}\epsilon^\sigma(L_z)\mathcal{R}'(0), \qquad (12)$$

$$\mathcal{T}^{\sigma\rho}_{J=0} \equiv \sum_{L_z,S_z}\langle 1, L_z; 1, S_z|0,0\rangle\;\epsilon^\sigma(L_z)\epsilon^\rho(S_z) = \sqrt{\frac{1}{3}}\left(g^{\sigma\rho} - \frac{P^\sigma P^\rho}{M^2}\right) \qquad (13)$$

QCD formalism

Our vertex (off-shell)

$$V_{J=0}^{c_1 c_2}(q_1, q_2) = 8ig^2 \frac{\delta^{c_1 c_2}}{M} \frac{\mathcal{R}'(0)}{\sqrt{\pi M N_c}}
\frac{3M^2(q_{1,t}q_{2,t}) + 2q_{1,t}^2 q_{2,t}^2 - (q_{1,t}q_{2,t})(q_{1,t}^2 + q_{2,t}^2)}{(M^2 - q_{1,t}^2 - q_{2,t}^2)^2}. \tag{14}$$

KMR vertex (on-shell)

$$\begin{aligned} V_{J=0}^{c_1 c_2}[M \gg q_{1,t},\, q_{2,t}] &\simeq 8ig^2 \delta^{c_1 c_2} \frac{\mathcal{R}'(0)}{M^3} \frac{1}{\sqrt{\pi M N_c}} \Big\{ 3(q_{1,t}q_{2,t}) \Big\} = \\ &= i\delta^{c_1 c_2} \cdot 8g^2 \sqrt{\frac{3}{\pi M}} \frac{\mathcal{R}'(0)}{M^3} \cdot (q_{1,t}q_{2,t}). \end{aligned} \tag{15}$$

Uncertainties for KMR UGDFs

- 1) $Q^2_{1,t} = \min(q^2_{0,t}, q^2_{1,t}), \;\; Q^2_{2,t} = \min(q^2_{0,t}, q^2_{2,t}) \quad ,$
- 2) $Q^2_{1,t} = \max(q^2_{0,t}, q^2_{1,t}), \;\; Q^2_{2,t} = \max(q^2_{0,t}, q^2_{2,t}) \quad ,$
- 3) $Q^2_{1,t} = q^2_{1,t}, \;\; Q^2_{2,t} = q^2_{2,t} \quad .$
- 4) $Q^2_{1,t} = q^2_{0,t}, \;\; Q^2_{2,t} = q^2_{0,t} \quad ,$
- 5) $Q^2_{1,t} = (q^2_{0,t} + q^2_{1,t})/2, \;\; Q^2_{2,t} = (q^2_{0,t} + q^2_{2,t})/2 \quad .$

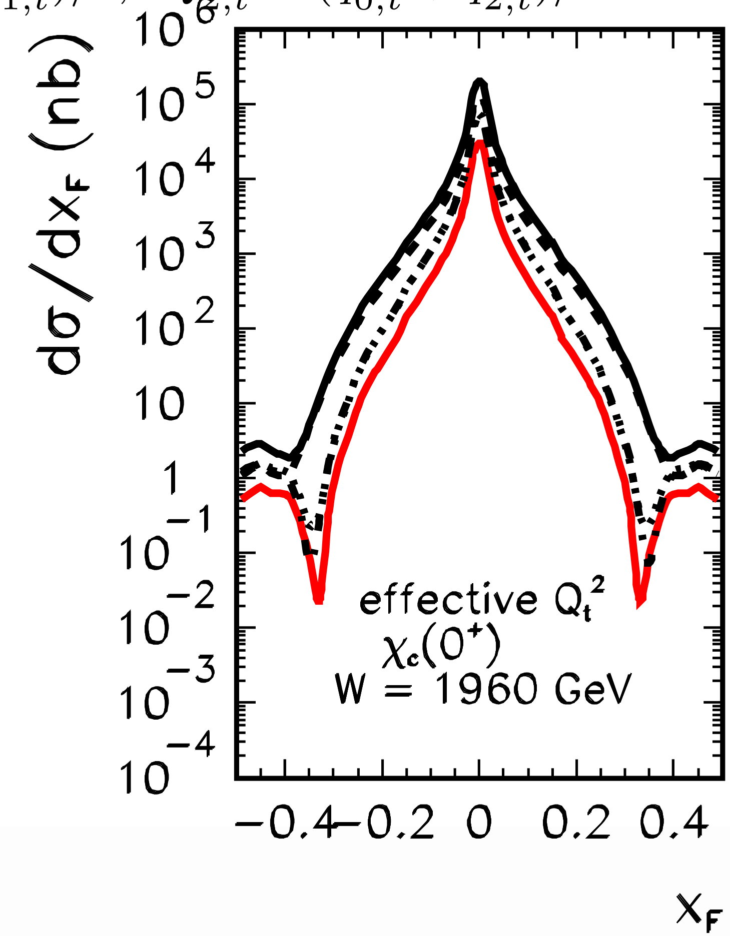

off-shell versus on-shell

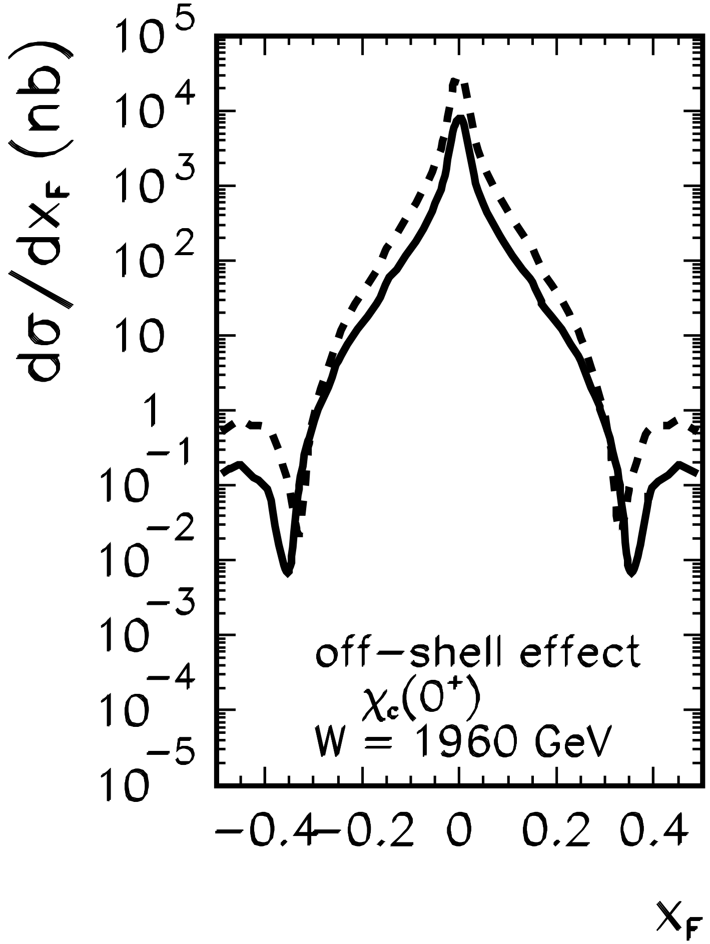

dashed line: on-shell, solid line: off-shell.

Diffractive production = central production

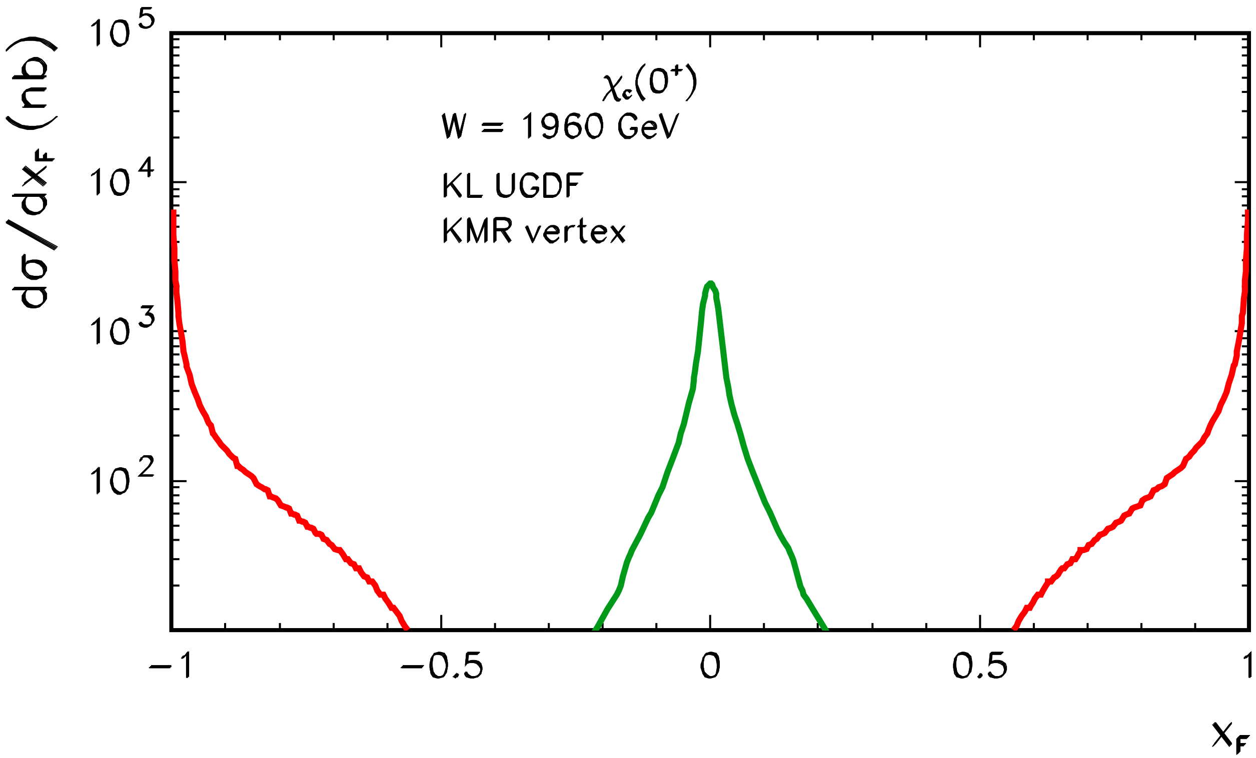

gap in longitudinal momenta between $\chi_c(0)$ and outgoing protons

Other UGDFs

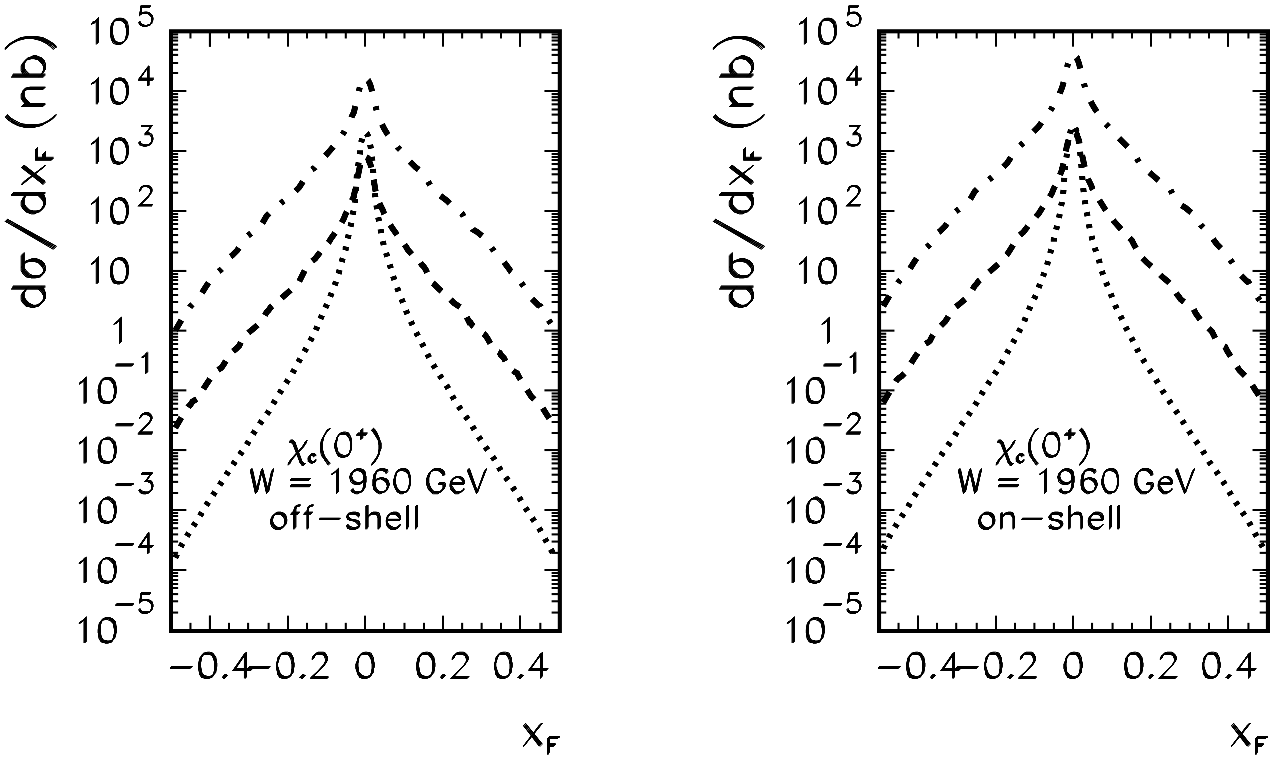

KL–dashed, GBW–dotted, BFKL–dash-dotted

Rapidity distribution

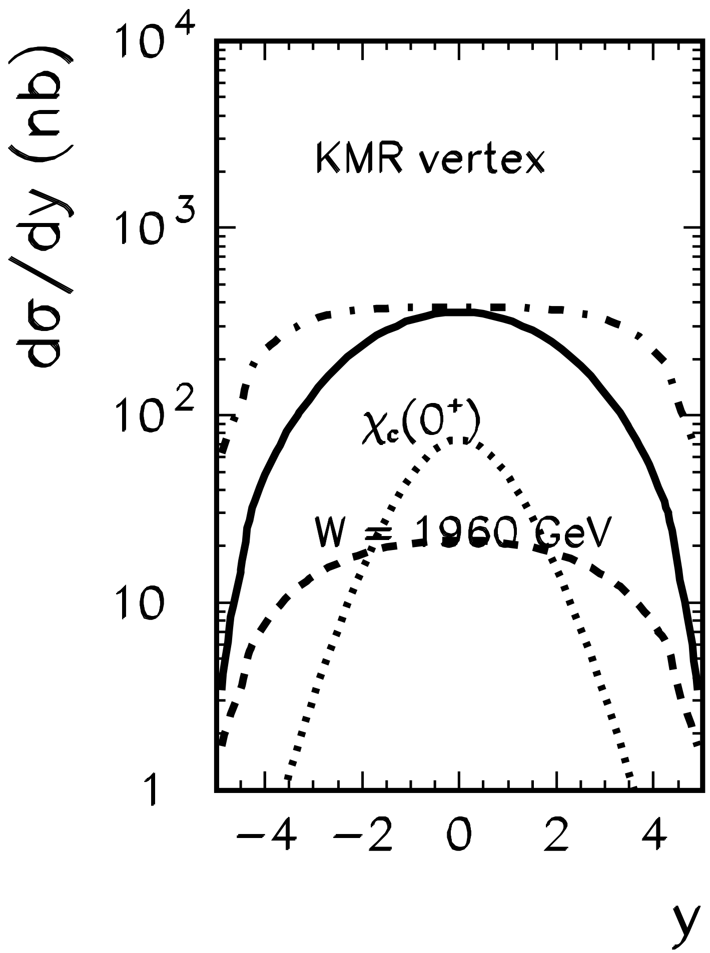

KL–dashed, GBW–dotted, BFKL–dash-dotted

Axial-vector $\chi_c(1^+)$

Landau-Yang theorem:

$$\mathcal{M}^{\lambda}_{\chi_c(1^+)\to gg}(k_1^2 = 0, k_2^2 = 0, p_M^2 = M_{\chi_c}^2) = 0 \; . \tag{16}$$

This means:

$$\Gamma_{\chi_c(1^+)\to gg} = 0 \; . \tag{17}$$

In our calculation, in the middle of diagram, gluons are off-shell and:

$$V^{\lambda}_{g^* g^* \to \chi_c(1^+)}(k_1^2 < 0, k_2^2 < 0, p_M^2 = M_{\chi_c}^2) \neq 0 \; . \tag{18}$$

$k_1^2 \approx -k_{1t}^2$ and $k_2^2 \approx -k_{2t}^2$

We have derived explicit formula for V and

$\mathcal{M}^{\lambda}_{pp\to pp\chi_c}(y, t_1, t_2, \phi)$.

$\sum_\lambda |V_\lambda|^2$ we reproduce formula of Kniehl-Vasin-Saleev,

used for inclusive production of $\chi_c(1^+)$.

$\chi_c(0^+)$ versus $\chi_c(1^+)$

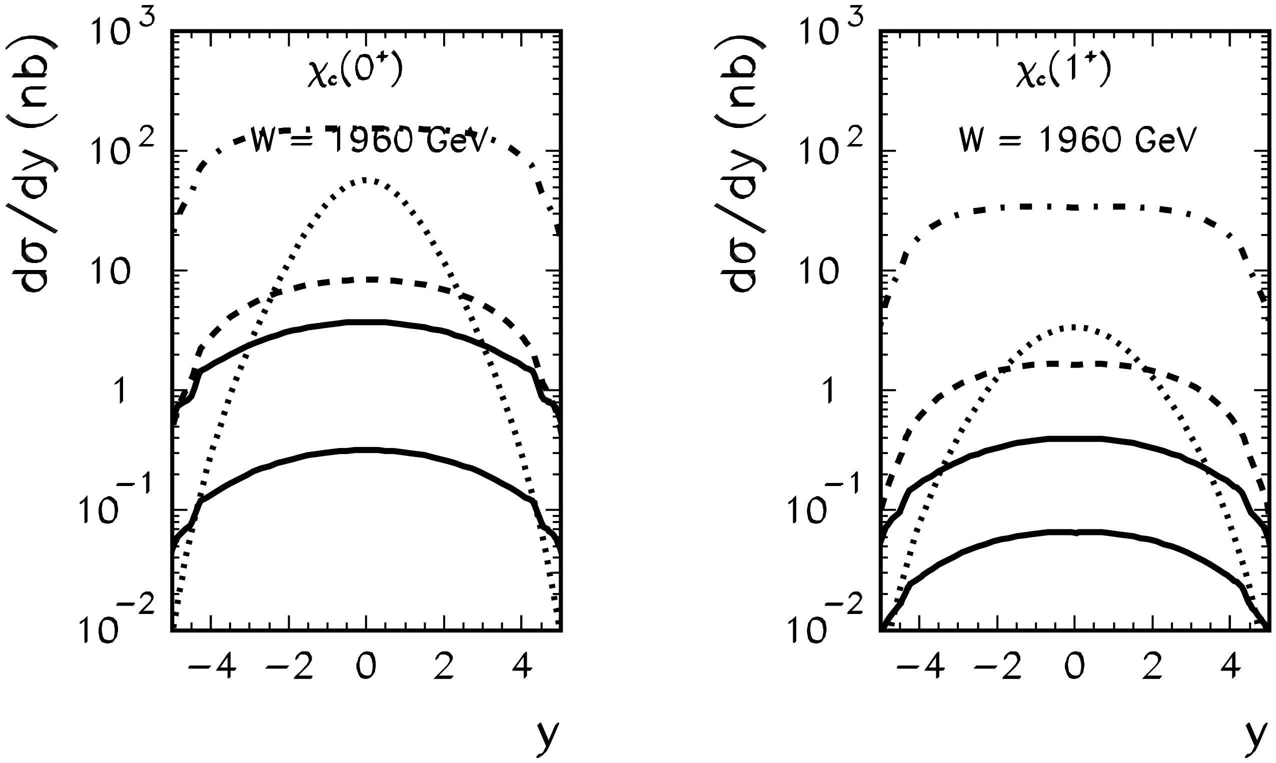

$$\sigma(\chi_c(0^+)) > \sigma(\chi_c(1^+))$$

$\chi_c(0^+)$ **versus** $\chi_c(1^+)$

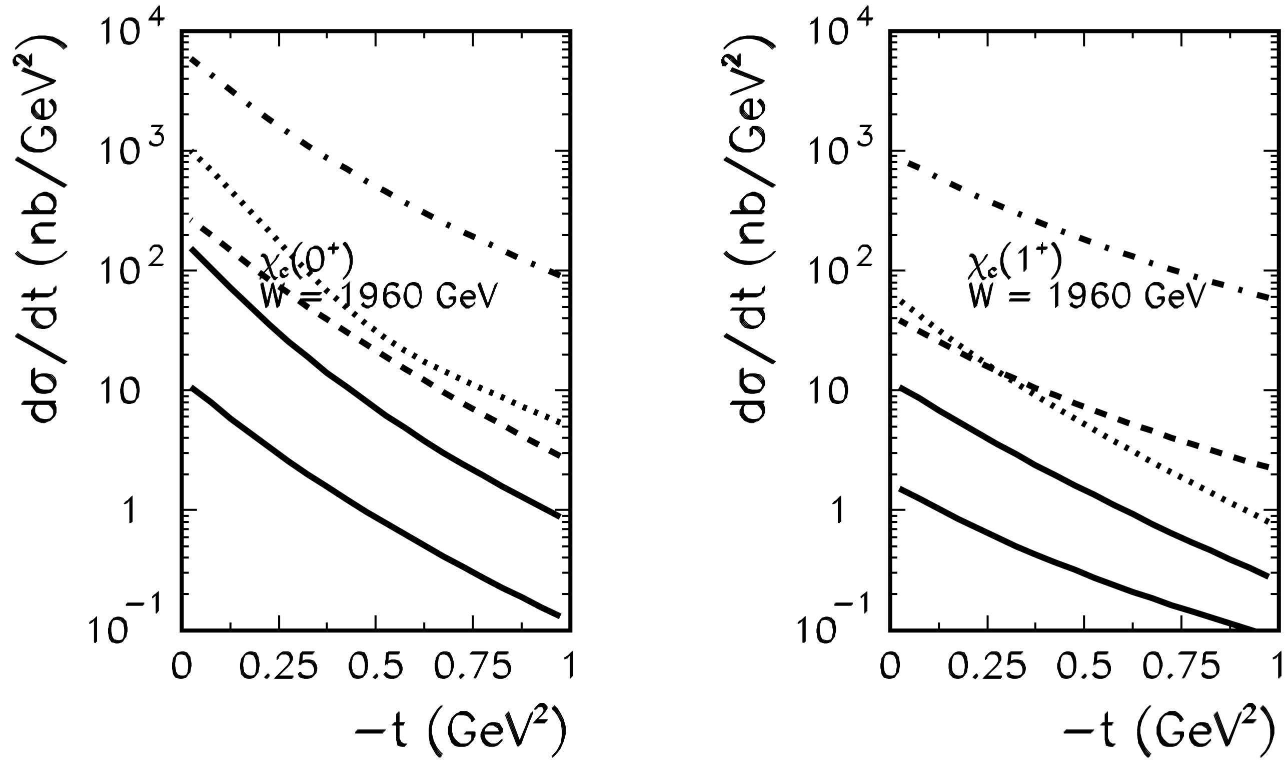

$$\sigma(\chi_c(0^+)) > \sigma(\chi_c(1^+))$$

$\chi_c(0^+)$ versus $\chi_c(1^+)$

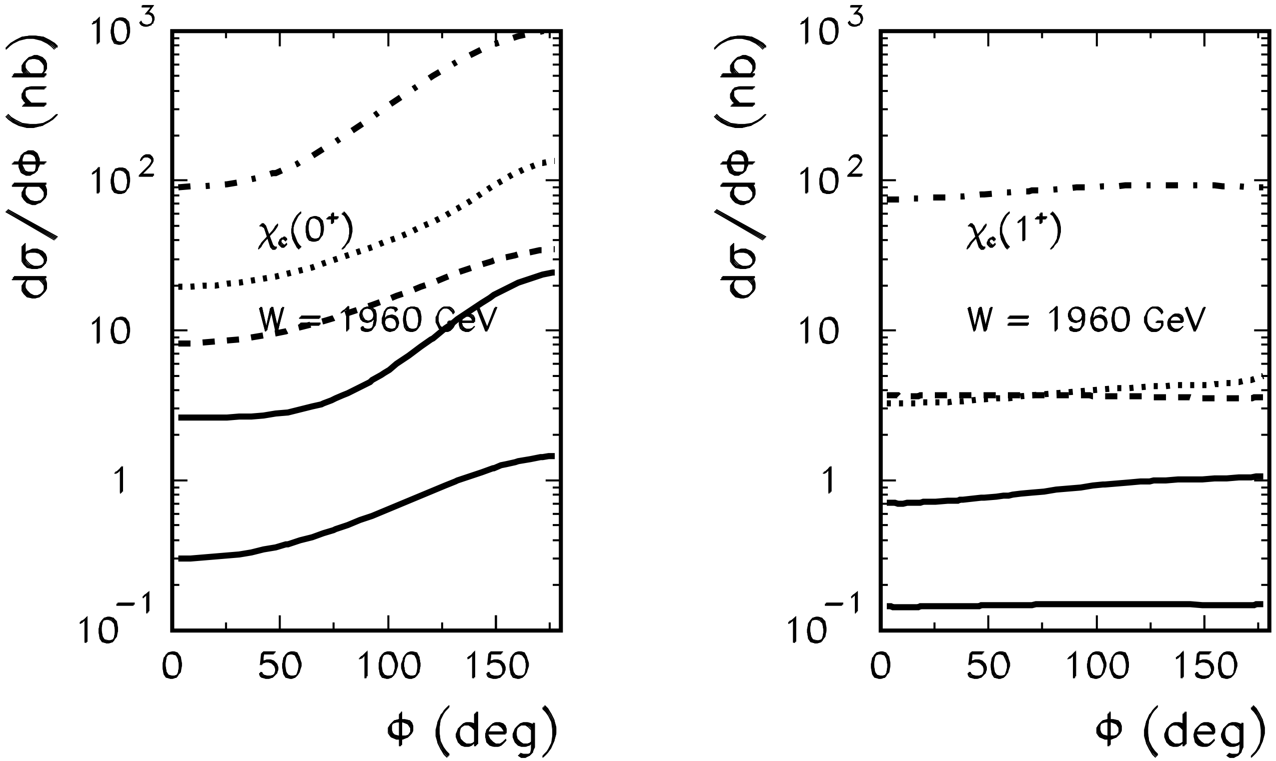

$$\sigma(\chi_c(0^+)) > \sigma(\chi_c(1^+))$$

$\chi_c(0^+)$ versus $\chi_c(1^+)$

Table 1: W = 1960 GeV

BR$(\chi_c(0^+) \to J/\Psi\,\gamma) = 0.0128$

BR$(\chi_c(1^+) \to J/\Psi\,\gamma) = 0.36$

UGDF	$\chi_c(0^+)$ σ_{tot}	$\chi_c(0^+)$ BR$\cdot\sigma_{tot}$	$\chi_c(1^+)$ σ_{tot}	$\chi_c(1^+)$ BR$\cdot\sigma_{tot}$	ratio $\frac{BR\cdot\sigma_{tot}(\chi_c(1^+))}{BR\cdot\sigma_{tot}(\chi_c(0^+))}$
KL	55.2	0.7	9.4	3.4	4.9
GBW	160	2	12.2	4.4	2.2
BFKL	1.2(+3)	15.4	272	98	6.4
Gauss, $\sigma_0 = 0.5$ GeV	26	0.3	2.8	1	3.3
Gauss, $\sigma_0 = 1.0$ GeV	2.2	0.03	0.5	0.2	6.7

CDF assumes that $\chi_c(0^+)$ dominates in the $\gamma + J/\Psi$ channel

Then $\sigma(\chi_c(0^+))$ can be extracted.

Summary of the χ_c part

- Big uncertainties in the Khoze-Martin-Ryskin approach.
- Huge sensitivity to the choice of UGDFs.
- Large off-shell effects.
- Different shapes for $\frac{d\sigma}{dx_F}$ ($\frac{d\sigma}{dy}$) for different UGDFs.
- Strong deviations from (1+cos(2 Φ)) for QCD diffraction.
- σ(photon-photon) $\ll$ σ(QCD diffraction).
- Different shapes of both components.
- Sizeable but not dominant contribution for exclusive J/ψ production via $\chi_c(0) \to J/\psi \gamma$.

Exclusive $f_0(1500)$ production in proton-proton and proton-antiproton collisions

P. Lebiedowicz and A.S.

Scalar glueball $f_0(1500)$ production

Many theoretical calculations (including lattice QCD) predicted existence of glueballs with $M > 1.5$ GeV.
$f_0(1500)$ is one of the candidates.

Short history:

- $f_0(1500)$ discovered by the Crystall Barrel Collaboration in proton-antiproton annihilation
- Observed by the WA102 Collaboration in central production $pp \to pp f_0(1500)$
- Observed at BES in $J/\psi \to f_0(1500) + \gamma$

Exclusive production of $f_0(1500)$

Close and Kirk – a phenomenological model.
In their language the pomerons (transverse and longitudinal) are the effective degrees of freedom.
The Close-Kirk amplitude:

$$\mathcal{M}(t_1, t_2, \phi') = a_T \exp\left(\frac{b_T}{2}(t_1 + t_2)\right) + a_L \frac{\sqrt{t_1 t_2}}{\mu^2} \exp\left(\frac{b_L}{2}(t_1 + t_2)\right) \; cos(\phi') \; . \quad (19)$$

Comment on their approach:

- No explicit $f_0(1500)$-rapidity,
- No absolute normalization.

Exclusive production of $f_0(1500)$

We consider processes:

$$
\begin{aligned}
& p + p \to p + f_0(1500) + p \ \ (J - PARC) \, , \\
& p + \bar{p} \to p + f_0(1500) + \bar{p} \ \ (PANDA) \, , \qquad (20) \\
& p + \bar{p} \to n + f_0(1500) + \bar{n} \ \ (PANDA) \, ,
\end{aligned}
$$

Our approach:

- Explicit rapidity dependence,
- Absolute normalization

Let us concentrate on 3.5 GeV $< W <$ 50 GeV

Our approach to exclusive $f_0(1500)$ production

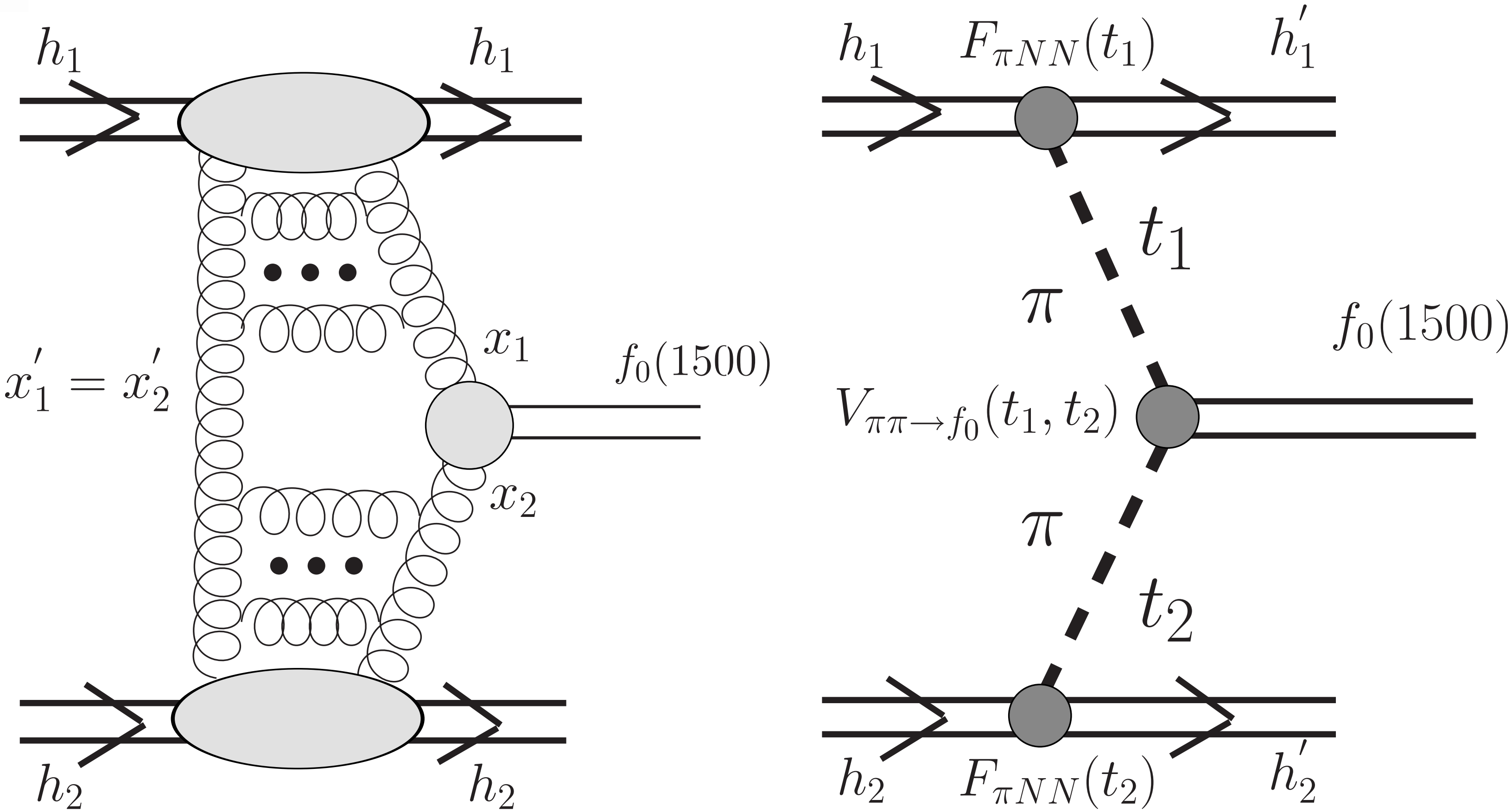

Figure 1: QCD mechanism vs MEC mechanism

Diffractive amplitude, part1

$$\mathcal{M}^{g^* g^*} = \frac{s}{2} \cdot \pi^2 \frac{1}{2} \frac{\delta_{c_1 c_2}}{N_c^2 - 1} \Im \int d^2 q_{0,t} V_J^{c_1 c_2} \frac{f^{off}_{g,1}(x_1, x_1', q_{0,t}^2, q_{1,t}^2, t_1) f^{off}_{g,2}(x_2, x_2', q_{0,t}^2, q_{2,t}^2, t_2)}{q_{0,t}^2 \, q_{1,t}^2 \, q_{2,t}^2} . \quad (2$$

In the original Khoze-Martin-Ryskin (KMR) approach the amplitude is written as

$$\mathcal{M} = N \int \frac{d^2 q_{0,t} P[f_0(1500)]}{q_{0,t}^2 q_{1,t}^2 q_{2,t}^2} f_g^{KMR}(x_1, x_1', Q_{1,t}^2, \mu^2; t_1) f_g^{KMR}(x_2, x_2', Q_{2,t}^2, \mu^2; t_2) \, , \tag{22}$$

where only one transverse momentum is taken into account somewhat arbitrarily as

$$Q_{1,t}^2 = \min\{q_{0,t}^2, q_{1,t}^2\} \, , \qquad Q_{2,t}^2 = \min\{q_{0,t}^2, q_{2,t}^2\} \, , \tag{23}$$

and the normalization factor N can be written in terms of the $f_0(1500) \to gg$ decay width.

Diffractive amplitude, part2

In the general case we do not know off-diagonal UGDFs. R.Pasechnik, O.Teryaev and A.S. proposed a prescription:

$$
\begin{aligned}
f_{g,1}^{off} &= \sqrt{f_g^{(1)}(x_1', q_{0,t}^2, \mu_0^2) \cdot f_g^{(1)}(x_1, q_{1,t}^2, \mu^2)} \cdot F_1(t_1)\,, \\
f_{g,2}^{off} &= \sqrt{f_g^{(2)}(x_2', q_{0,t}^2, \mu_0^2) \cdot f_g^{(2)}(x_2, q_{2,t}^2, \mu^2)} \cdot F_1(t_2)\,, \quad (24)
\end{aligned}
$$

where $F_1(t_1)$ and $F_1(t_2)$ are isoscalar nucleon form factors.

$$
F_1(t_{1,2}) = \frac{4m_p^2 - 2.79\, t_{1,2}}{(4m_p^2 - t_{1,2})(1 - t_{1,2}/071)^2}\,. \quad (25)
$$

Even at intermediate energies (W = 10-50 GeV) typical $x_1' = x_2'$ are relatively small ($\sim$ 0.01). $x_1, x_2 \sim M_{f_0}/\sqrt{s}$ are not too small (typically $> 10^{-1}$). Therefore here we cannot use the small-x models of UGDFs.

Diffractive amplitude, part3

Gaussian smearing of the collinear distribution seems a reasonable solution:

$$\mathcal{F}_g^{Gauss}(x, k_t^2, \mu_F^2) = x g^{coll}(x, \mu_F^2) \cdot f_{Gauss}(k_t^2) \; , \tag{26}$$

where $g^{coll}(x, \mu_F^2)$ are standard collinear (integrated) gluon distribution and $f_{Gauss}(k_t^2)$ is a Gaussian two-dimensional function

$$f_{Gauss}(k_t^2) = \frac{1}{2\pi\sigma_0^2} \exp\left(-k_t^2/2\sigma_0^2\right)/\pi \; . \tag{27}$$

Above σ_0 is a free parameter. Summarizing, we propose:

$$f(x, x', k_t^2, k_t'^2, t) = \sqrt{f_{small-x}(x', k_t'^2) f_{Gauss}(x, k_t^2, \mu^2)} \cdot F(t) \; , \tag{28}$$

where $f_{small-x}(x', k_t'^2)$ is one of the typical small-x UGDFs.

Pion-pion MEC amplitude

$$
\begin{aligned}
\overline{|\mathcal{M}|^2} = \frac{1}{4} \quad & \left[(E_1+m)\left(E_1'+m\right)\left(\frac{\mathbf{p}_1^2}{(E_1+m)^2}+\frac{\mathbf{p}_1^{\prime 2}}{(E_1'+m)^2}-\frac{2\mathbf{p}_1\cdot\mathbf{p}_1'}{(E_1+m)(E_1'+m)}\right)\right]\cdot 2 \\
& \frac{g_{\pi NN}^2 \quad \cdot T_k}{(t_1-m_\pi^2)^2} F_{\pi NN}^2(t_1) \;\cdot\; |C_{f_0(1500)\to\pi\pi}|^2 \; V_{\pi\pi\to f_0(1500)}^2(t_1,t_2) \;\cdot\; \frac{g_{\pi NN}^2 \quad \cdot T_k}{(t_2-m_\pi^2)^2} F_{\pi N}^2 \\
& \left[(E_2+m)\left(E_2'+m\right)\left(\frac{\mathbf{p}_2^2}{(E_2+m)^2}+\frac{\mathbf{p}_2^{\prime 2}}{(E_2'+m)^2}-\frac{2\mathbf{p}_2\cdot\mathbf{p}_2'}{(E_2+m)(E_2'+m)}\right)\right]\cdot 2
\end{aligned}
$$

.

$g_{\pi NN}$ is the pion nucleon coupling constant ($\frac{g_{\pi NN}^2}{4\pi}$ = 13.5)
The isospin factor T_k equals 1 for the $\pi^0\pi^0$ fusion and equals 2 for the $\pi^+\pi^-$ fusion.
In the case of $p-p$ collisions only $\pi^0\pi^0$ fusion. In the case of $p-\bar{p}$ collisions both $\pi^0\pi^0$ and $\pi^+\pi^-$.

Pion-pion MEC amplitude

In central heavy meson production – large t_1 and t_2 $\rightarrow$ extended nature of the particles involved. This is incorporated via $F_{\pi NN}(t_1)$ or $F_{\pi NN}(t_2)$.
The normalization constant $|C|^2$ can be calculated from the partial decay width

$$|C_{f_0(1500)\to\pi\pi}|^2 = \frac{8\pi \; 2M_{f_0}^2 \Gamma_{f_0(1500)\to\pi^0\pi^0}}{\sqrt{M_{f_0}^2 - 4m_\pi^2}} \,, \tag{30}$$

where $\Gamma_{f_0(1500)\to\pi^0\pi^0} = 0.109 \cdot BR(f_0(1500) \to \pi\pi) \cdot 0.5$ GeV.
The branching ratio is $BR(f_0(1500) \to \pi\pi)$ = 0.349 (PDG).
The off-shellness of pions is also included for the $\pi\pi \to f_0(1500)$ transition through the extra $V_{\pi\pi\to f_0(1500)}(t_1, t_2)$ form factor.

Diffractive component, part1

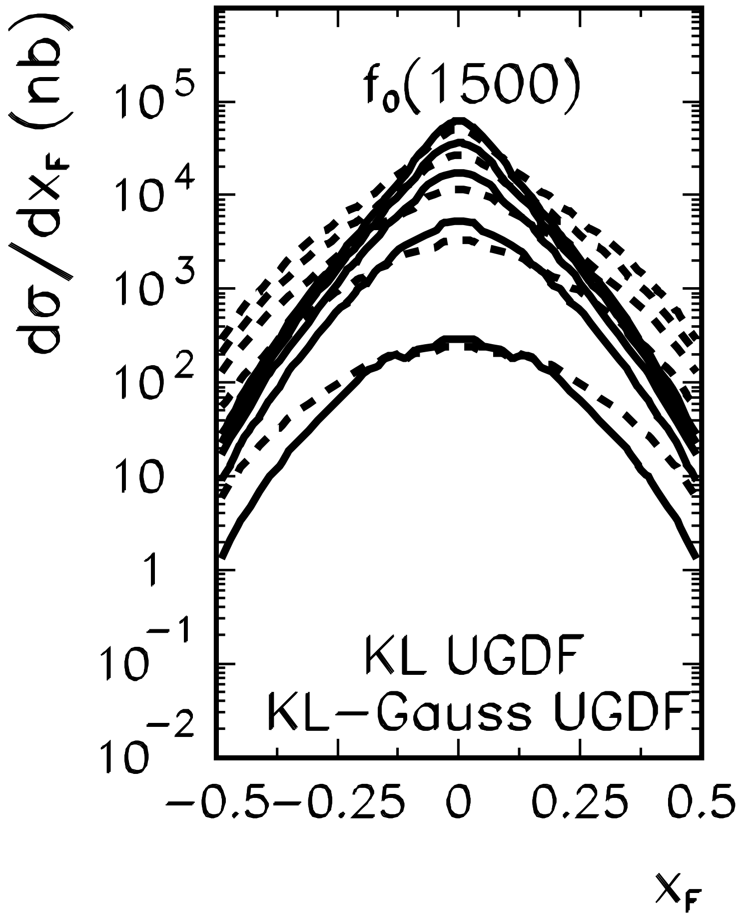

W = 10, 20, 30, 40, 50 GeV. Kharzeev-Levin UGDF (solid line) and the mixed distribution KL$\otimes$ Gauss (dashed line).

Diffractive component, part2

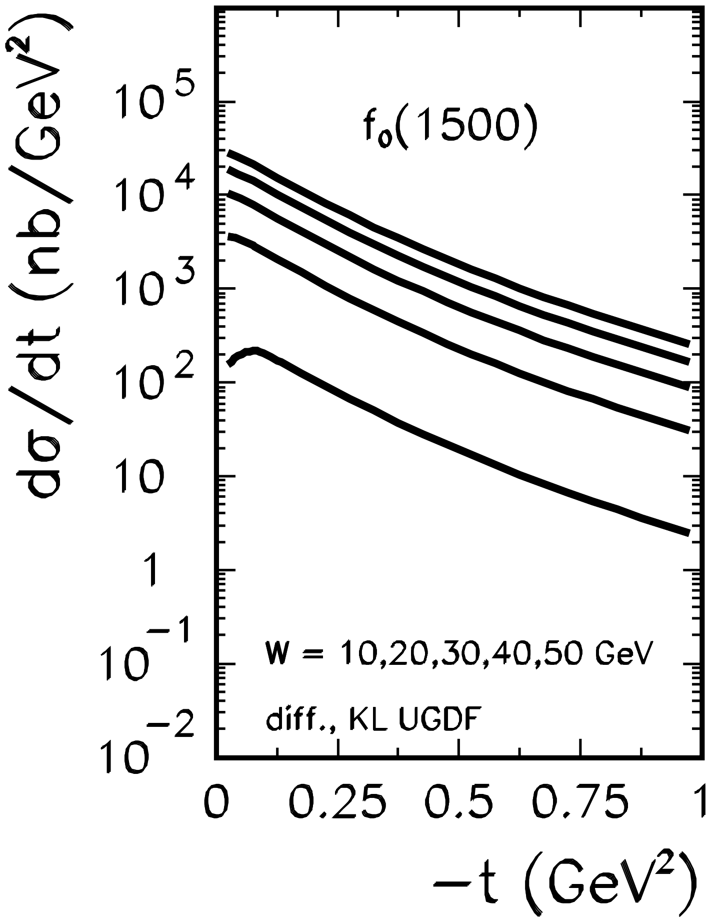

$t = t_1 = t_2$. Kharzeev-Levin UGDF.
$W = 10$, 20, 30, 40, 50 GeV.

Diffractive component, part3

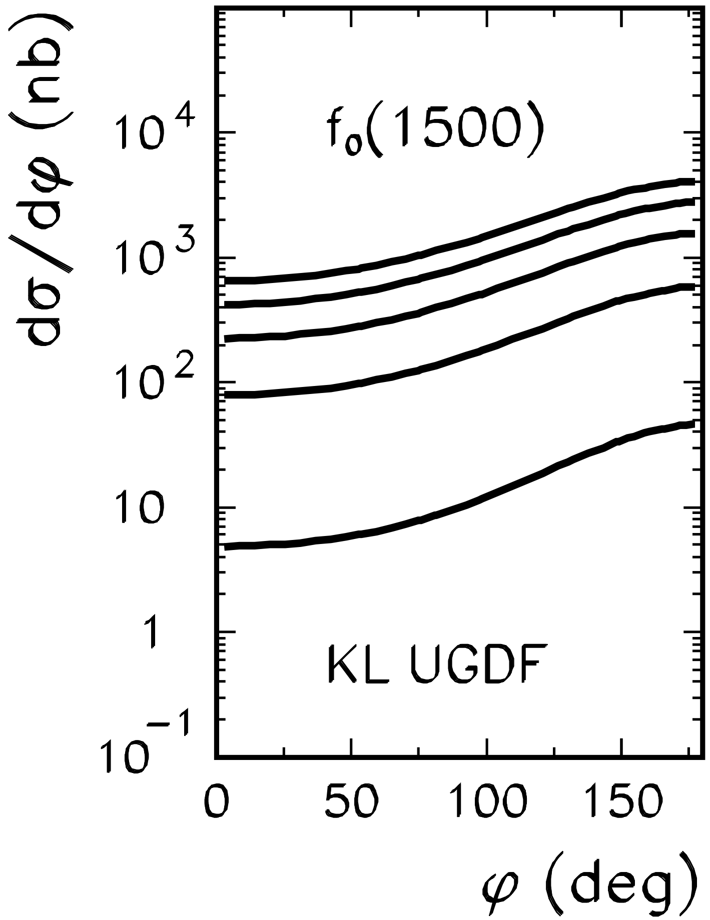

W = 10, 20, 30, 40, 50 GeV. KL UGDF.

Energy dependence

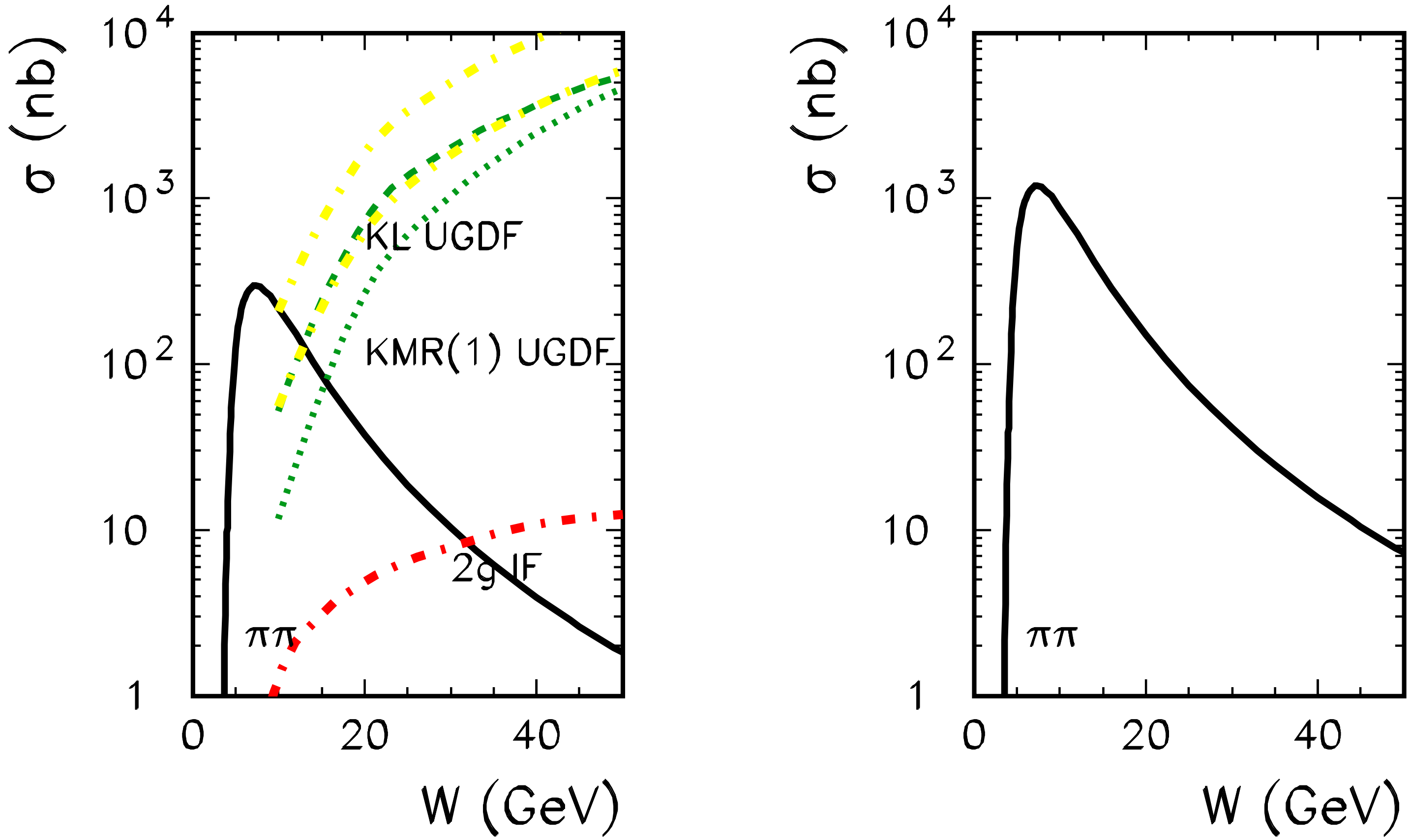

$p\bar{p} \to p\bar{p} f_0(1500)$ (left panel) and $p\bar{p} \to n\bar{n} f_0(1500)$ (right panel).

Momentum transfer

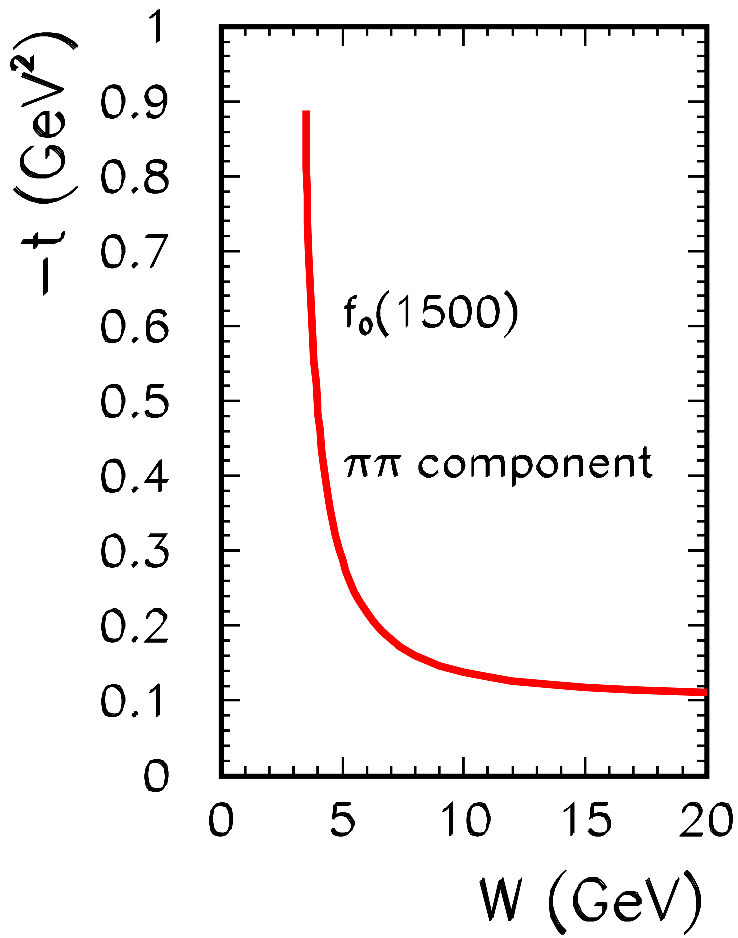

Average value of $< t_1 > = < t_2 >$.

Predictions for PANDA, part1

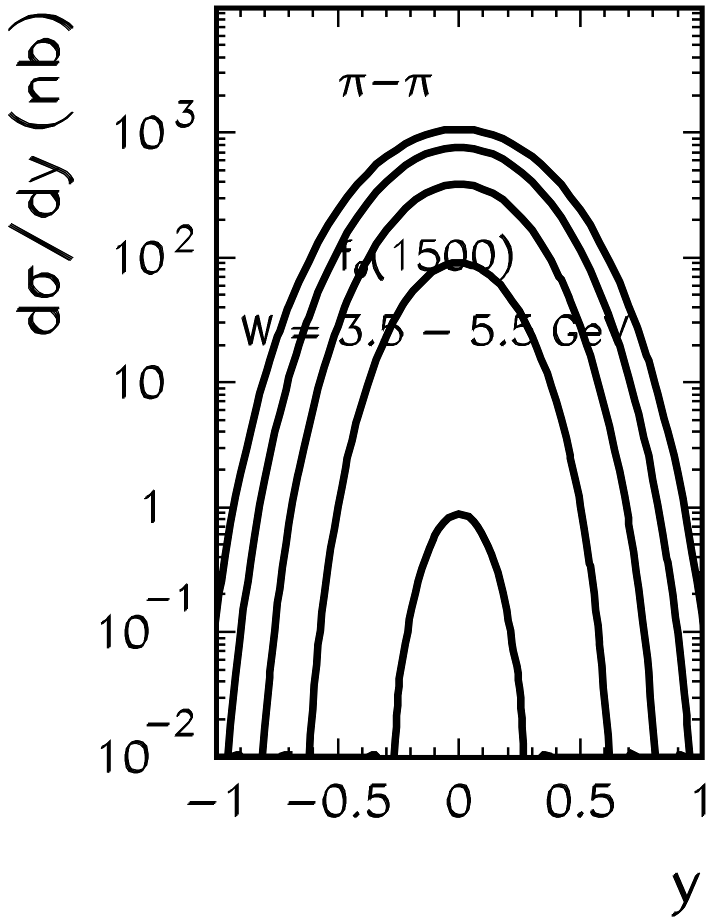

$p\bar{p} \to n\bar{n} f_0(1500)$. W = 3.5, 4.0, 4.5, 5.0, 5.5 GeV.

Predictions for PANDA, part2

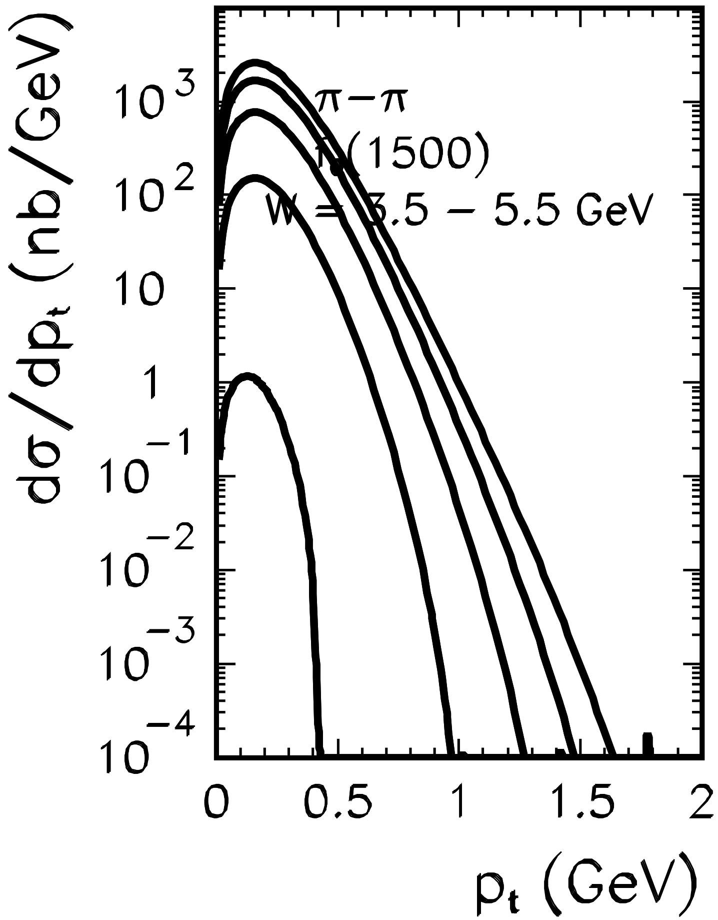

Transverse momentum distribution of neutrons or antineutrons. $p\bar{p} \to n\bar{n} f_0(1500)$. W = 3.5, 4.0, 4.5, 5.0, 5.5 GeV.

Predictions for PANDA, part3

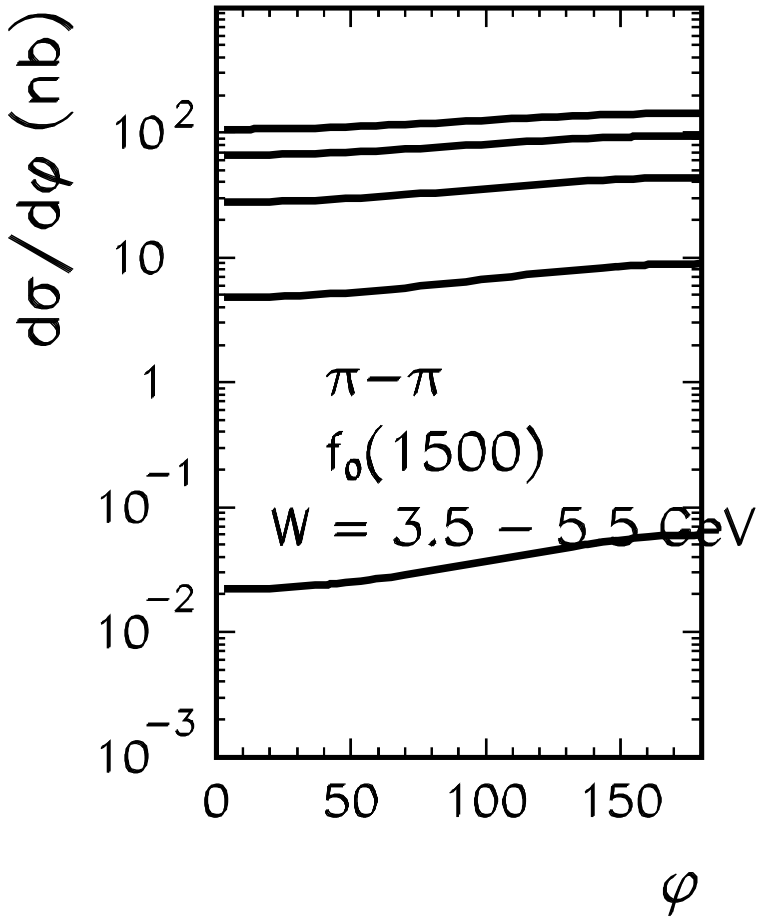

Azimuthal angle between neutron and antineutron in the reaction $p\bar{p} \to n\bar{n} f_0(1500)$. W = 3.5, 4.0, 4.5, 5.0, 5.5 GeV.

Helicity decomposition

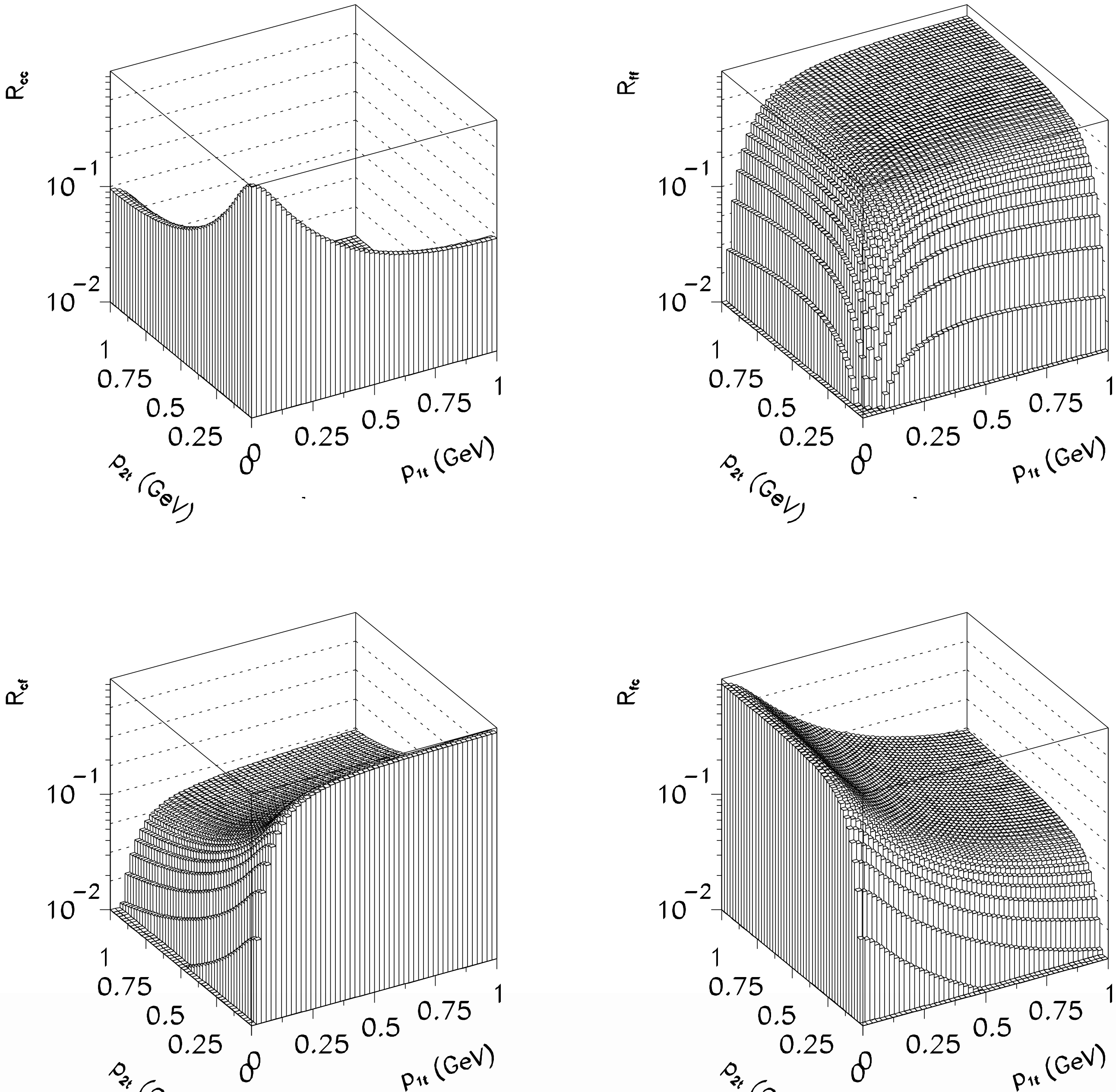

Background to $f_0(1500)$ production for PANDA

Select $\pi^+\pi^-$ decay channel

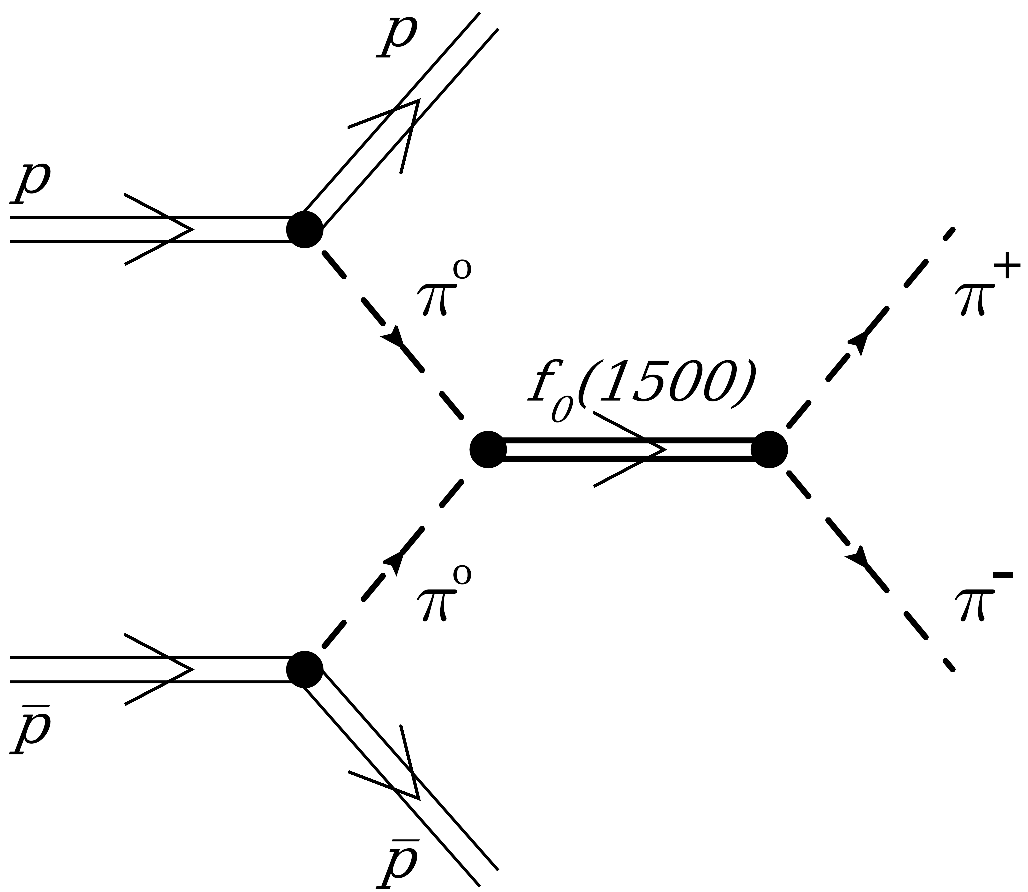

four-body final state !!!

Background to $f_0(1500)$ production for PANDA

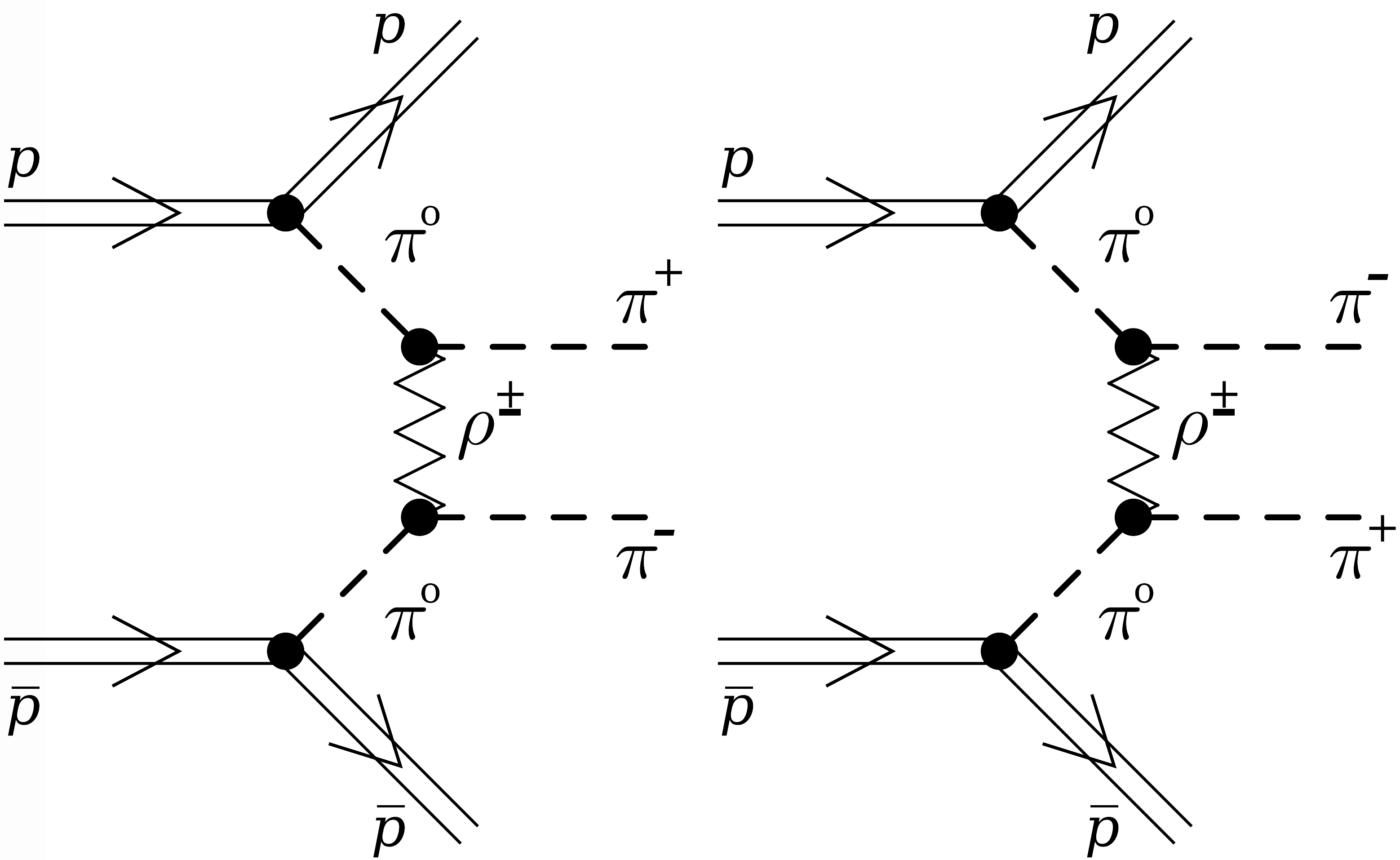

Background to $f_0(1500)$ production for PANDA

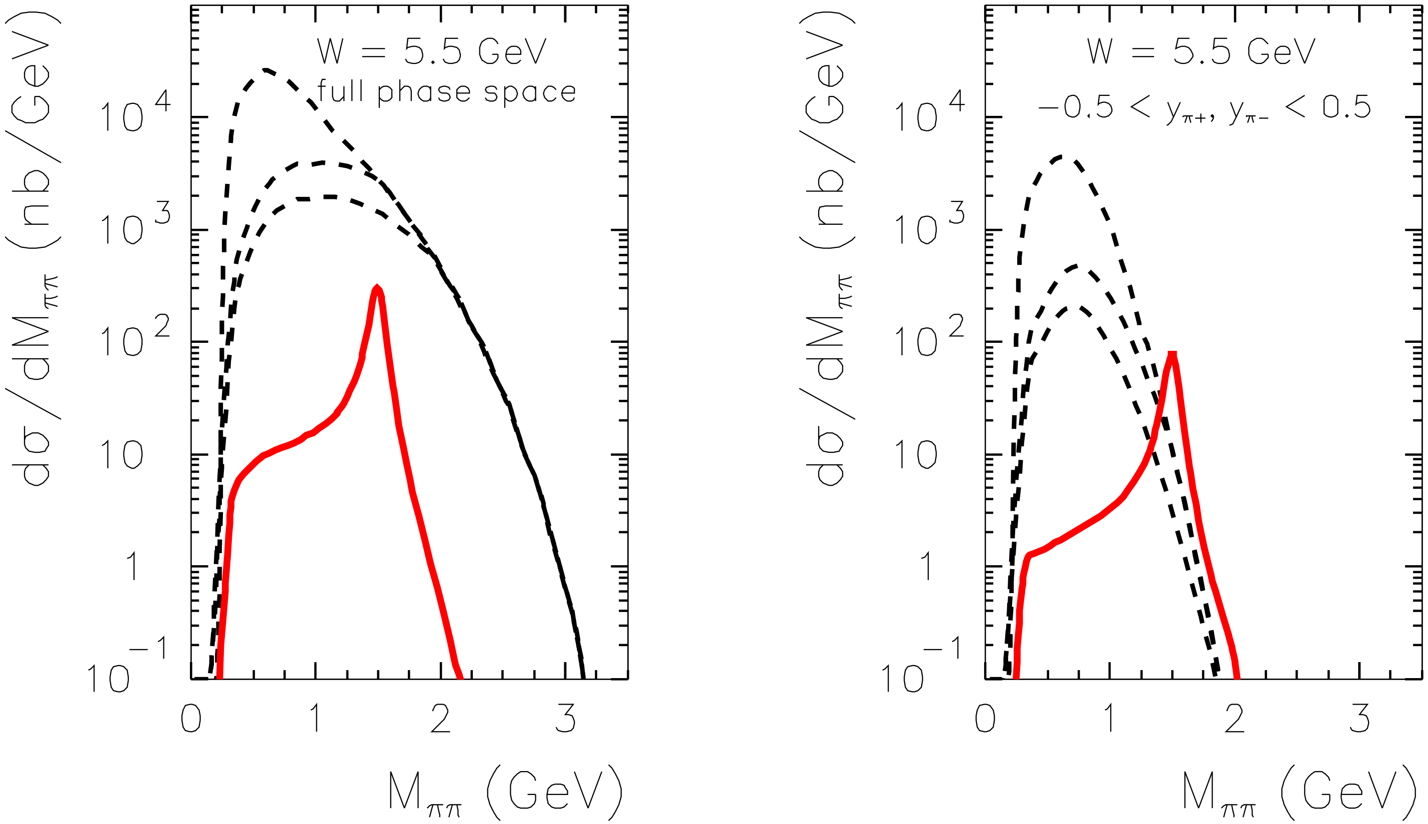

-0.5 $< y_{\pi^+}, y_{\pi^-} <$ 0.5

New mechanism of $f_0(1500)$ production

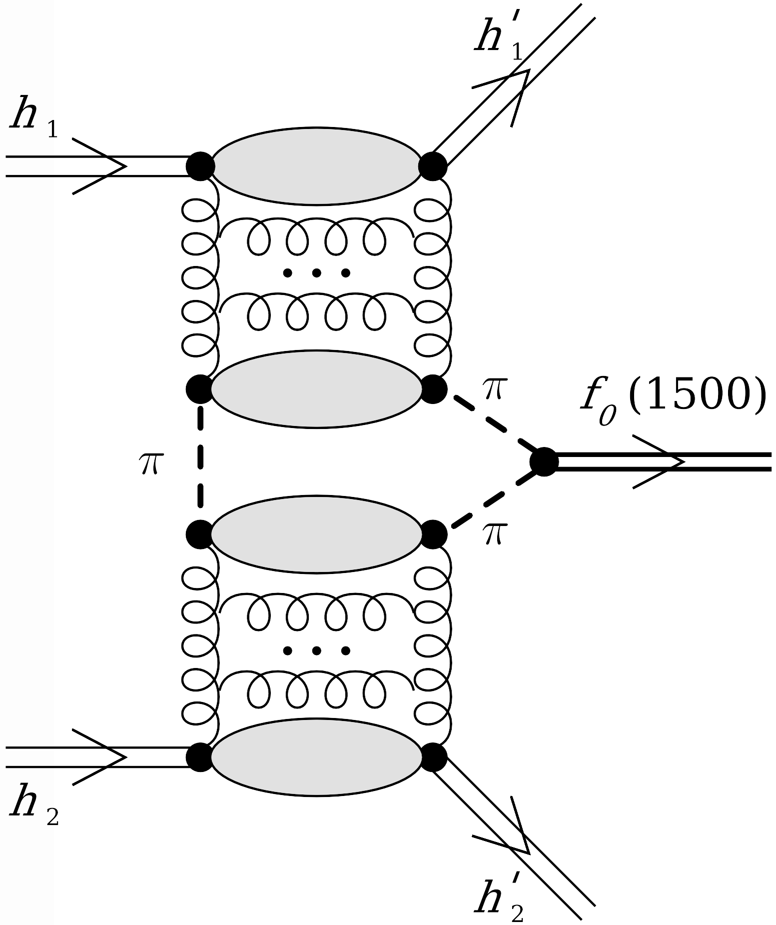

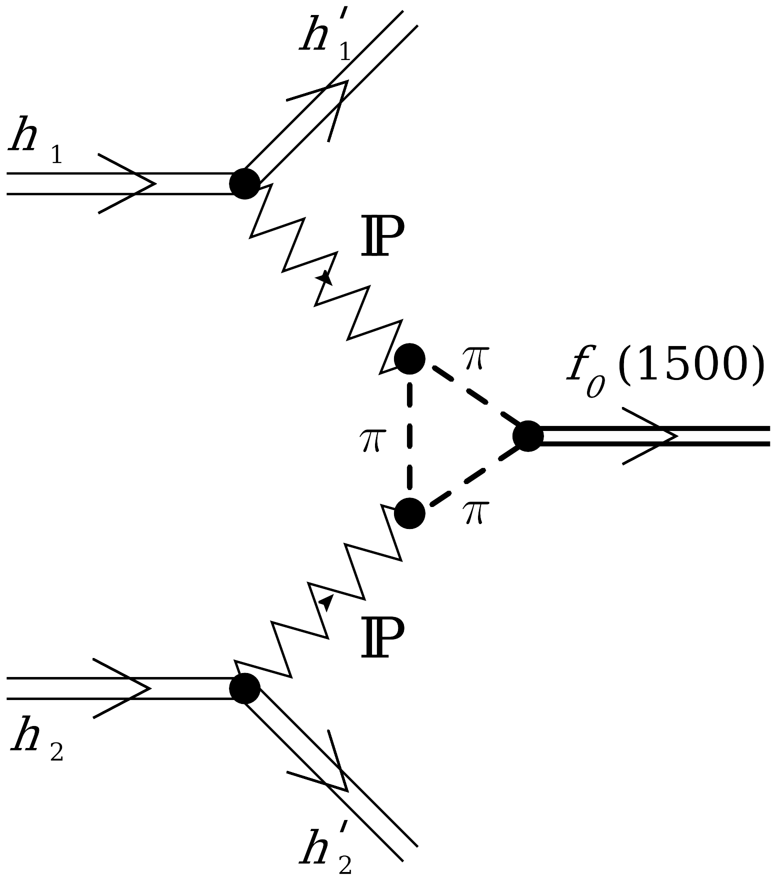

New mechanism of $f_0(1500)$ production

$$\mathcal{M}_{\lambda_1\lambda_2\to\lambda_1'\lambda_2'}(y,p_{1t},p_{2t},\phi) =$$

$$\delta_{\lambda_1\lambda$$

$$\left(F_{ppIP}(t_1) i s_1 C_{\pi p}^{IP}\left(\frac{s_1}{s_0}\right)^{\alpha_{IP}(t_1)-1} F_{\pi\pi IP}(t_1) + F_{ppIR}(t_1)\eta_f s_1 C_{\pi p}^{IR}\left(\frac{s_1}{s_0}\right)^{\alpha_{IR}(t_1)-1} F_{\pi\pi IR}(t_1)\right)$$

$$T_{IPIPf_0}(q_1,q_2,p_{f_0}$$

$$\left(F_{\pi\pi IP}(t_2) i s_2 C_{\pi p}^{IP}\left(\frac{s_2}{s_0}\right)^{\alpha_{IP}(t_2)-1} F_{ppIP}(t_2) + F_{\pi\pi IR}(t_2)\eta_f s_2 C_{\pi p}^{IR}\left(\frac{s_2}{s_0}\right)^{\alpha_{IR}(t_2)-1} F_{ppIR}(t_2)\right)$$

$$\delta_{\lambda_2\lambda_2'}$$

$$T_{IPIPf_0}(q_1,q_2,p_{f_0}) = \int \frac{d^4k}{(2\pi)^4}\Bigg(F(q_1,k_1,k)\,\frac{1}{(q_1-k)^2-m_\pi^2+i\epsilon}$$

$$F(q_2,k_2,k)\,\frac{1}{(q_2+k)^2-m_\pi^2+i\epsilon}$$

$$F(k_1,k_2,p_{f_0})\; g_{\pi\pi f_0}\;\frac{1}{k^2-m_\pi^2+i\epsilon}\;.$$

Vertex form factors

Exponential form factors:

$$F(q_1, k_1, k) = \exp\left(-|k_1^2 - m_\pi^2|/{\Lambda_E}^2\right) \cdot \exp\left(-|k^2 - m_\pi^2|/{\Lambda_E}^2\right) \;,$$

$$F(q_2, k_2, k) = \exp\left(-|k_2^2 - m_\pi^2|/{\Lambda_E}^2\right) \cdot \exp\left(-|k^2 - m_\pi^2|/{\Lambda_E}^2\right) \;,$$

$$F(k_1, k_2, p_{f_0}) = \exp\left(-|k_1^2 - m_\pi^2|/{\Lambda_E}^2\right) \cdot \exp\left(-|k_2^2 - m_\pi^2|/{\Lambda_E}^2\right) \;. \quad (32)$$

Λ_E = 1 GeV

We also tried Gaussian form factors

New mechanism of $f_0(1500)$ production

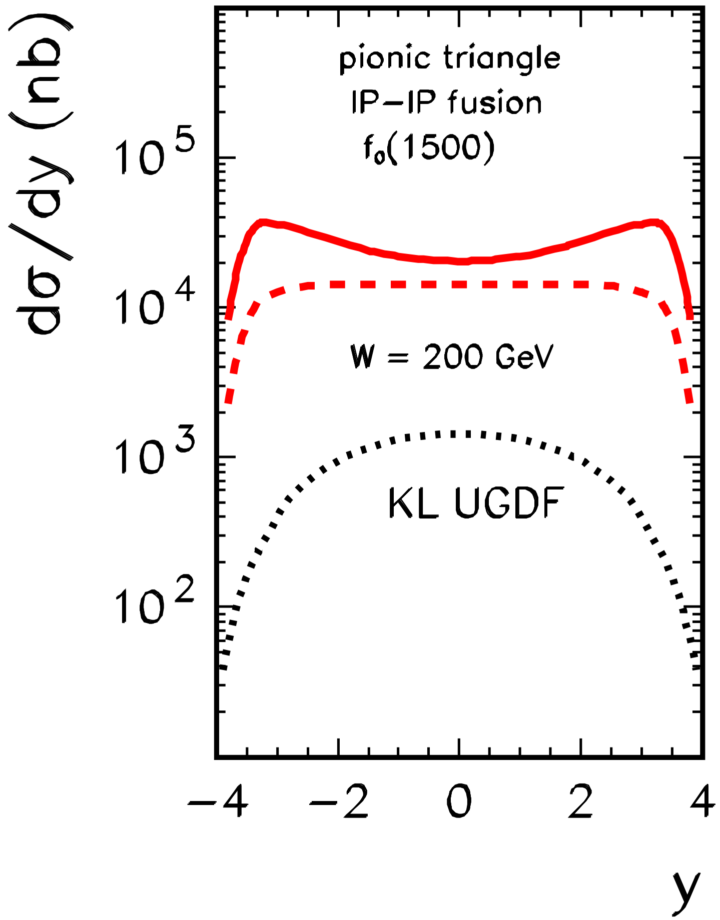

Λ_E = 1 GeV

HUGE CROSS SECTION!!!

Summary of the glueball part

- We have estimated differential cross section for exclusive $f_0(1500)$ production.
- Diffractive QCD mechanism (dominance at higher energies) and pion-pion fusion (dominance close to threshold).
- Experiments with PANDA and at J-PARC(?) could verify the predictions.
- Simultaneous analysis of:
  (a) $pp \to pp f_0(1500)$
  (b) $p\bar{p} \to p\bar{p} f_0(1500)$
  (c) $p\bar{p} \to n\bar{n} f_0(1500)$
  would help to disantangle the mechanism of the reaction.
- $f_0(1500) \to \pi\pi$. Continuum in the $\pi\pi$ channel?
- Planning experiments requires a dedicated Monte Carlo simulation of the apparatus.

Exclusive Υ production in proton-proton and proton-antiproton collisions

A. Rybarska, W. Schäfer and A. Szczurek

Introduction

- Exclusive production of heavy $Q\bar{Q}$ vector quarkonium states in hadronic interactions was never measured
- We restrict only to photon-Pomeron, Pomeron-photon fusion mechanism
- The current experimental analyses at the Tevatron call for an evaluation of differential distributions including the effect of absorptive corrections
- The HERA data for $\gamma p \to \Upsilon p$ cover only energy range $W \sim$ 100 - 200 GeV. This energy range is relevant to the exclusive production at Tevatron energies for not too large rapidities of the meson

Diagram for exclusive $\gamma p \longrightarrow \Upsilon p$

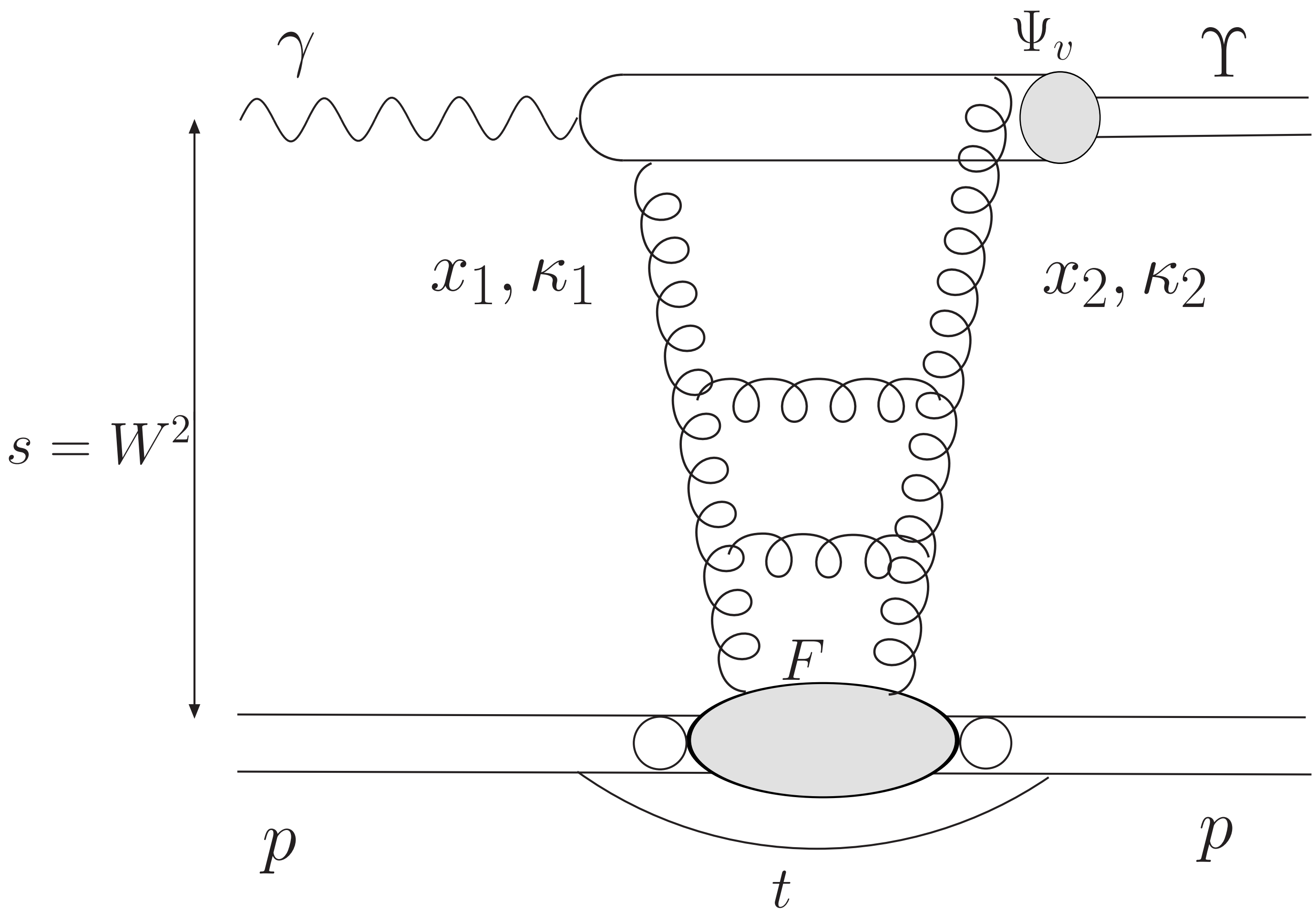

see Ivanov-Nikolaev-Savin

Imaginary part of the amplitude for γp $\longrightarrow$ Υp

$$\Im m\, \mathcal{M}(W,\Delta^2=0,Q^2=0) = W^2 \frac{c_\Upsilon \sqrt{4\pi\alpha_{em}}}{4\pi^2}\, 2\int_0^1 \frac{dz}{z(1-z)} \int_0^\infty \pi dk^2 \psi_V(z,$$

$$\int_0^\infty \frac{\pi d\kappa^2}{\kappa^4}\alpha_S(q^2)\mathcal{F}(x_{eff},\kappa^2)\Big(A_0(z,k^2)\, W_0(k^2,\kappa^2)+A_1(z,k^2)\, W_1(k^2,\kappa^2$$

where

$$\begin{aligned}
A_0(z,k^2) &= m_b^2 + \frac{k^2 m_b}{M+2m_b} \\
A_1(z,k^2) &= \left[z^2+(1-z)^2-(2z-1)^2\frac{m_b}{M+2m_b}\right]\frac{k^2}{k^2+m_b^2},
\end{aligned}$$

$$\begin{aligned}
W_0(k^2,\kappa^2) &= \frac{1}{k^2+m_b^2} - \frac{1}{\sqrt{(k^2-m_b^2-\kappa^2)^2+4m_b^2k^2}} \\
W_1(k^2,\kappa^2) &= 1-\frac{k^2+m_b^2}{2k^2}\left(1+\frac{k^2-m_b^2-\kappa^2}{\sqrt{(k^2-m_b^2-\kappa^2)^2+4m_b^2k^2}}\right).
\end{aligned}$$

Total cross section for γp $\longrightarrow$ Υp

The full amplitude:

$$\mathcal{M}(W,\Delta^2) = (i+\rho)\,\Im m\mathcal{M}(W,\Delta^2=0)\,\exp(-B(W)\Delta^2)\,.$$

where

$$\rho = \frac{\Re e\mathcal{M}}{\Im m\mathcal{M}} = \frac{\pi}{2}\frac{\partial\log\left(\Im m\mathcal{M}/W^2\right)}{\partial\log W^2} = \frac{\pi}{2}\Delta_{\mathbb{P}}\,.$$

$$B(W) = B_0 + 2\alpha'_{eff}\log\left(\frac{W^2}{W_0^2}\right)\,,$$

with: $\alpha'_{eff} = 0.164$ GeV^{-2}, $W_0 = 95$ GeV (H1 Collaboration, 2006)

Total cross section can be written as:

$$\sigma_{tot}(\gamma p \to Vp) = \frac{1+\rho^2}{16\pi B(W)}\left|\Im m\frac{\mathcal{M}(W,\Delta^2)}{W^2}\right|^2$$

Parameters of the Υ wave function

Υ decay electronic width:

$$\Gamma(V \to e^+e^-) = \frac{4\pi\alpha_{em}^2 c_\Upsilon}{3M_V^3} \cdot g_V^2 \cdot K_{NLO}$$

Leading-order approximation:

$$K_{NLO} = 1$$

Next-to-leading-order approximation:

$$K_{NLO} = 1 - \frac{16}{3\pi}\alpha_S(m_b^2)$$

g_v -leptonic decay constant:

$$g_V = \frac{8N_c}{3}\int \frac{d^3\vec{p}}{(2\pi)^3}(M+m_b)\,\psi_V(p^2)$$

1) $\Gamma(V \to e^+e^-) \Rightarrow g_V$ and this depends on K_{NLO}

2) $g_V \Rightarrow$ parameters of $\psi_V(p^2)$

The ratio of the cross sections $\Upsilon(2S)/\Upsilon(1S)$

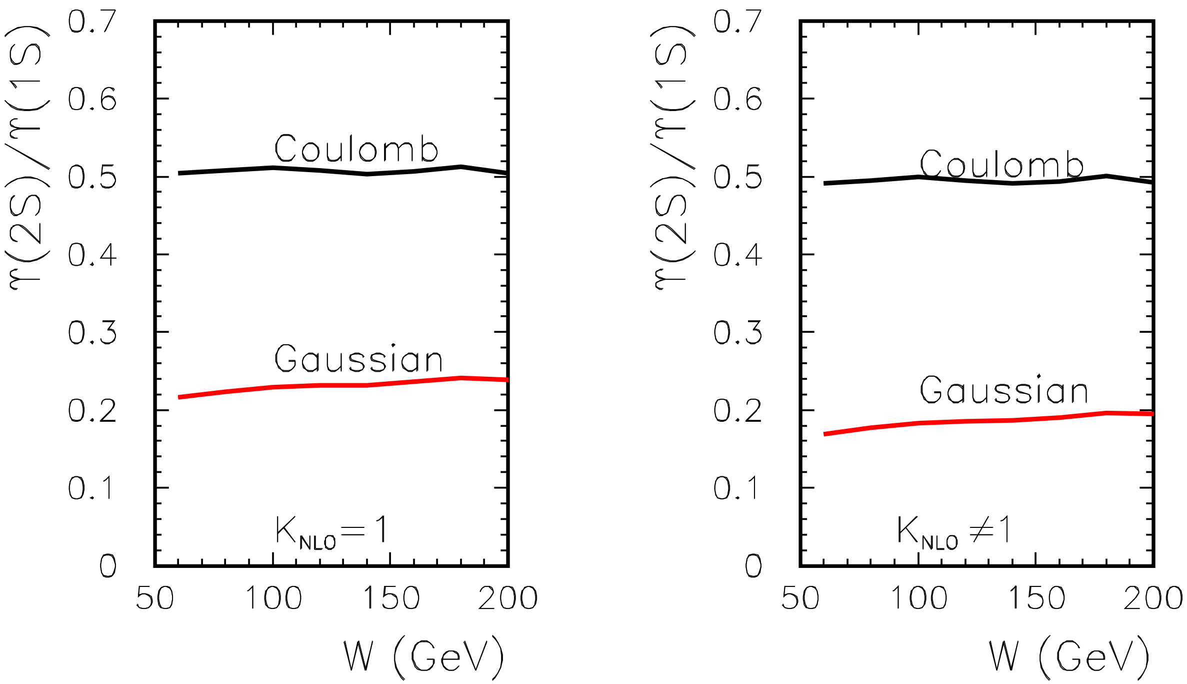

Gaussian wave function:

$$\psi_{1S}(p^2) = C_1 \exp\left(-\frac{p^2 a_1^2}{2}\right) \,,\ \psi_{2S}(p^2) = C_2(\xi_0 - p^2 a_2^2) \exp\left(-\frac{p^2 a_2^2}{2}\right) \,,$$

Coulomb wave function:

$$\psi_{1S}(p^2) = \frac{C_1}{\sqrt{M}} \frac{1}{(1+a_1^2 p^2)^2} \,,\ \psi_{2S}(p^2) = \frac{C_2}{\sqrt{M}} \frac{\xi_0 - a_2^2 p^2}{(1+a_2^2 p^2)^3} \,.$$

Total cross section for $\gamma p \longrightarrow \Upsilon p$

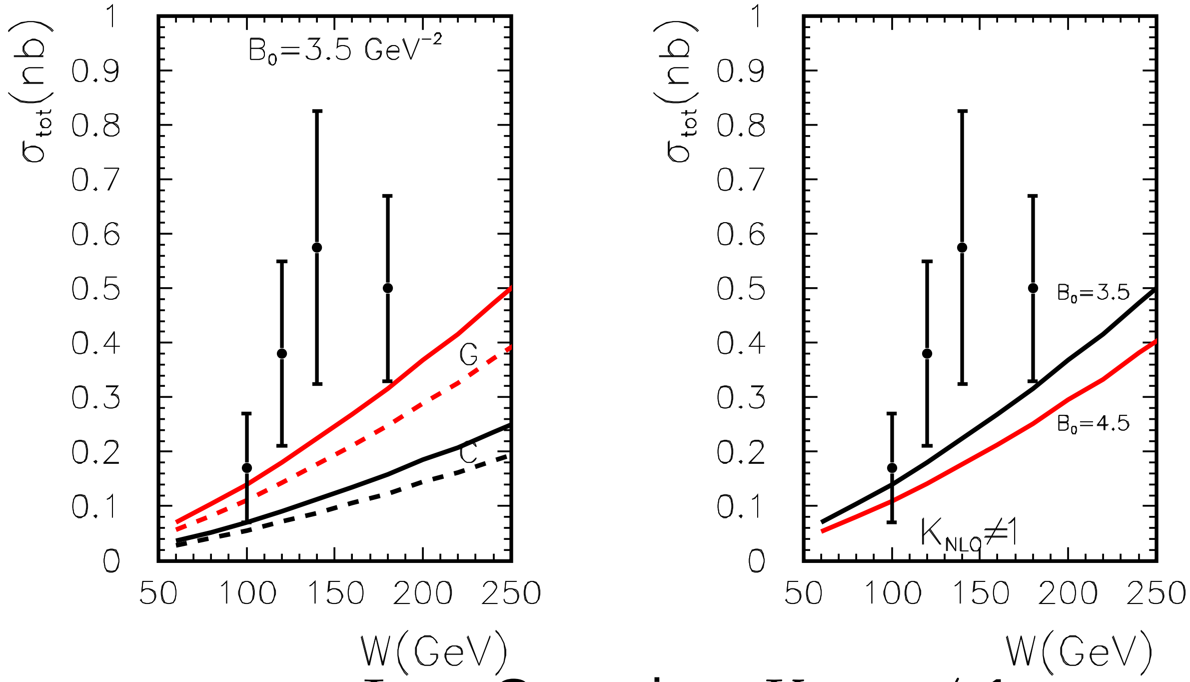

$\Psi_V -$ Gaussian, $K_{NLO} \neq 1$

$\Psi_V -$ Gaussian, $K_{NLO} = 1$

$\Psi_V -$ Coulomb, $K_{NLO} \neq 1$

$\Psi_V -$ Coulomb, $K_{NLO} = 1$

Dominant bare mechanism for $p\bar{p} \longrightarrow p\bar{p}\,\Upsilon$

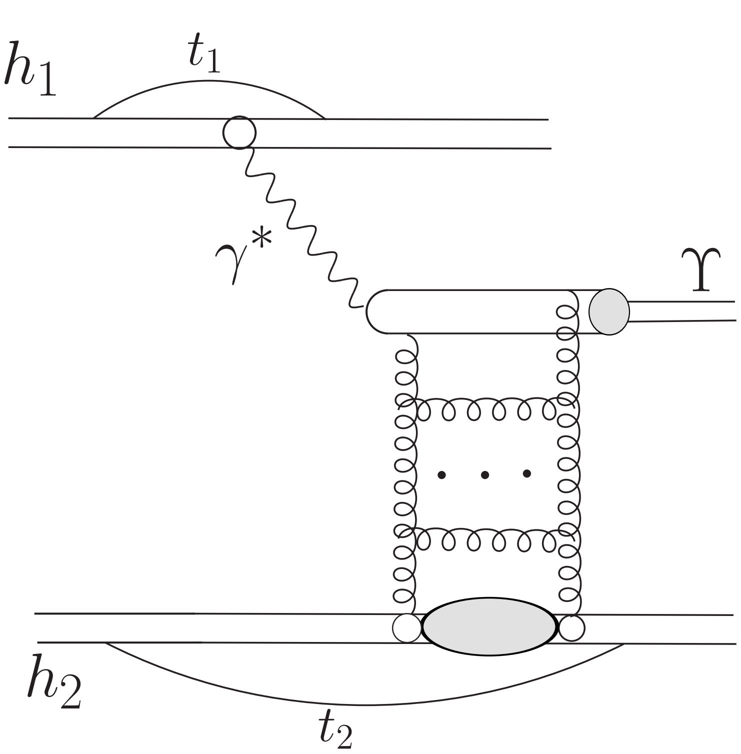

photon-pomeron

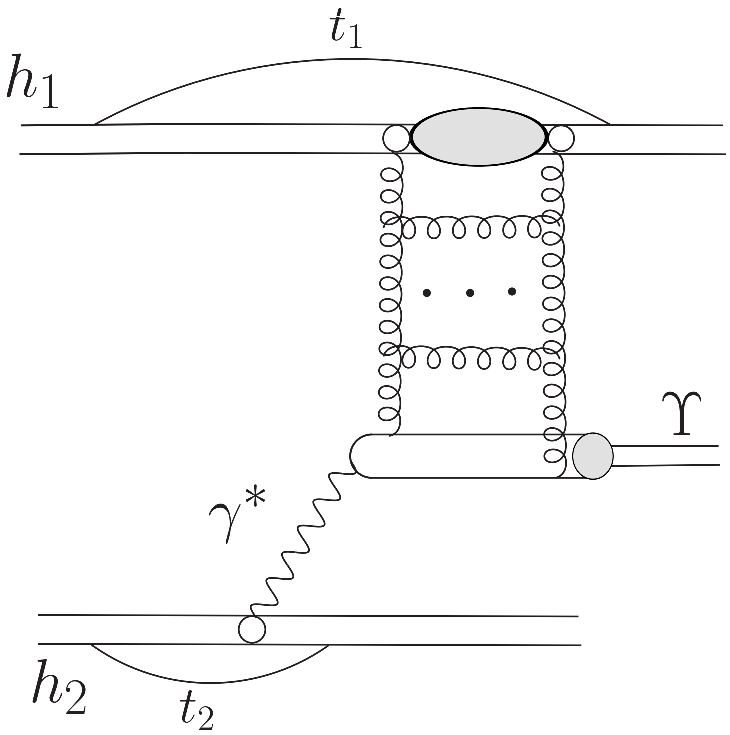

pomeron-photon

also pomeron-odderon (odderon-pomeron) diagrams
(Bzdak, Motyka, Szymanowski)

Diagram for $p\bar{p} \longrightarrow p\bar{p}\,\Upsilon$ with absorptive correc

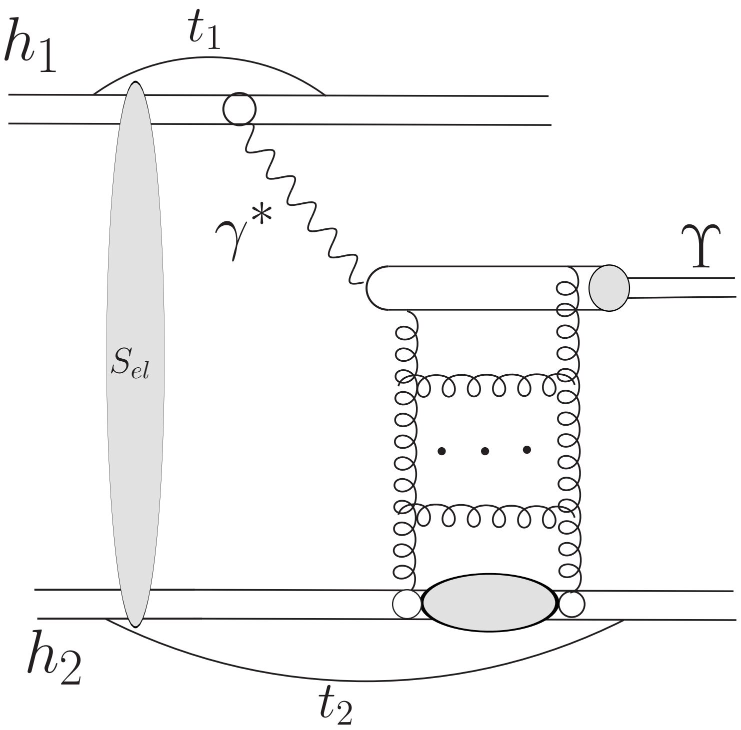

photon-pomeron

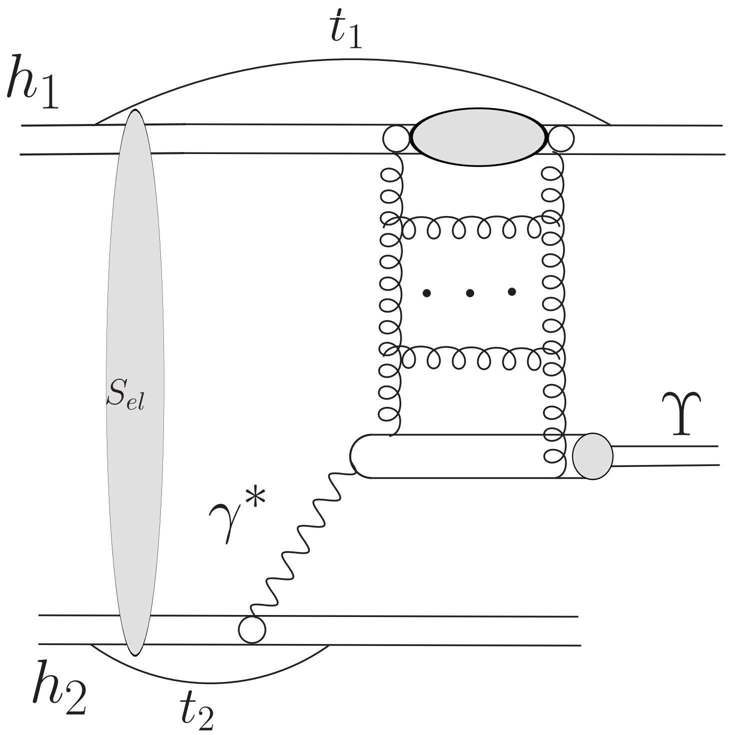

pomeron-photon

Amplitude for $p\bar{p} \longrightarrow p\bar{p}\,\Upsilon$

Amplitude without absorption:

$$\begin{aligned}
\boldsymbol{M}^{(0)}(\boldsymbol{p}_1,\boldsymbol{p}_2) &= e_1 \frac{2}{z_1}\frac{\boldsymbol{p}_1}{t_1}\mathcal{F}_{\lambda_1'\lambda_1}(\boldsymbol{p}_1,t_1)\mathcal{M}_{\gamma^* h_2 \to V h_2}(s_2,t_2,Q_1^2) \\
&+ e_2 \frac{2}{z_2}\frac{\boldsymbol{p}_2}{t_2}\mathcal{F}_{\lambda_2'\lambda_2}(\boldsymbol{p}_2,t_2)\mathcal{M}_{\gamma^* h_1 \to V h_1}(s_1,t_1,Q_2^2)\,,
\end{aligned}$$

Full amplitude for $p\bar{p} \longrightarrow p\bar{p}\,\Upsilon$:

$$\begin{aligned}
\boldsymbol{M}(\boldsymbol{p}_1,\boldsymbol{p}_2) &= \int \frac{d^2\boldsymbol{k}}{(2\pi)^2}\, S_{el}(\boldsymbol{k})\, \boldsymbol{M}^{(0)}(\boldsymbol{p}_1-\boldsymbol{k},\boldsymbol{p}_2+\boldsymbol{k}) \\
&= \boldsymbol{M}^{(0)}(\boldsymbol{p}_1,\boldsymbol{p}_2) - \delta\boldsymbol{M}(\boldsymbol{p}_1,\boldsymbol{p}_2)\,,
\end{aligned}$$

where

$$S_{el}(\boldsymbol{k}) = (2\pi)^2\delta^{(2)}(\boldsymbol{k}) - \frac{1}{2}T(\boldsymbol{k})\ ,\ \ T(\boldsymbol{k}) = \sigma_{tot}^{pp}(s)\,\exp\Big(-\frac{1}{2}B_{el}\boldsymbol{k}^2\Big)\,,$$

Cross section for exclusive photoproduction in

The absorptive correction for amplitude :

$$\delta \boldsymbol{M}(\boldsymbol{p}_1, \boldsymbol{p}_2) = \int \frac{d^2\boldsymbol{k}}{2(2\pi)^2} \, T(\boldsymbol{k}) \, \boldsymbol{M}^{(0)}(\boldsymbol{p}_1 - \boldsymbol{k}, \boldsymbol{p}_2 + \boldsymbol{k}) \, .$$

The differential cross section is given in terms of $\boldsymbol{M}$ as

$$d\sigma = \frac{1}{512\pi^4 s^2} |\boldsymbol{M}|^2 \, dy dt_1 dt_2 d\phi \, ,$$

where

- y is rapidity of the vector meson
- ϕ is azimuthal angle between $\boldsymbol{p}_1$ and $\boldsymbol{p}_2$

$d\sigma/dy$ for $\Upsilon(1S)$ and $\Upsilon(2S)$

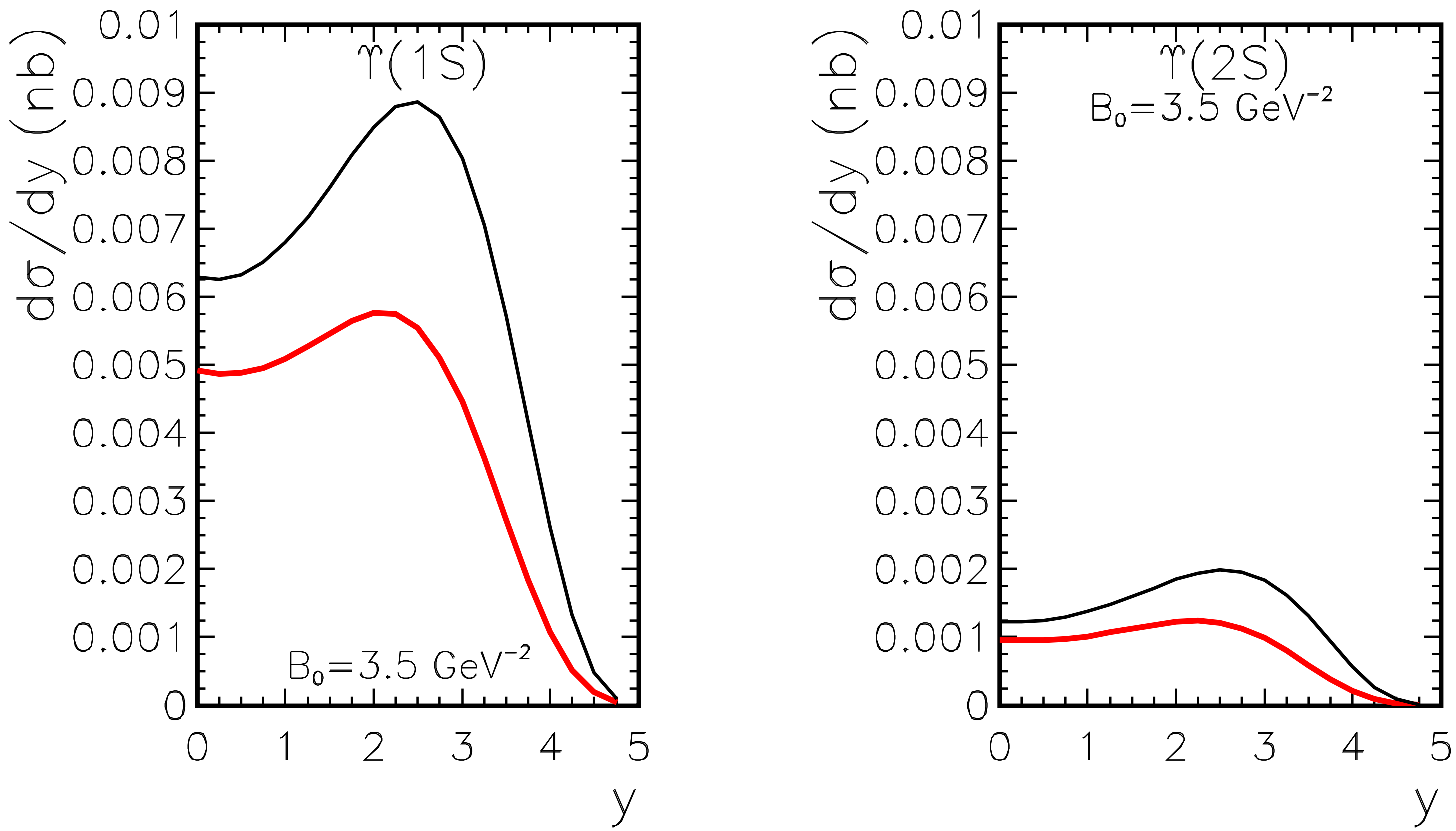

with absorption

without absorption

$d\sigma/dydp_t^2$ as a function of p_t^2 for Υ(1S)

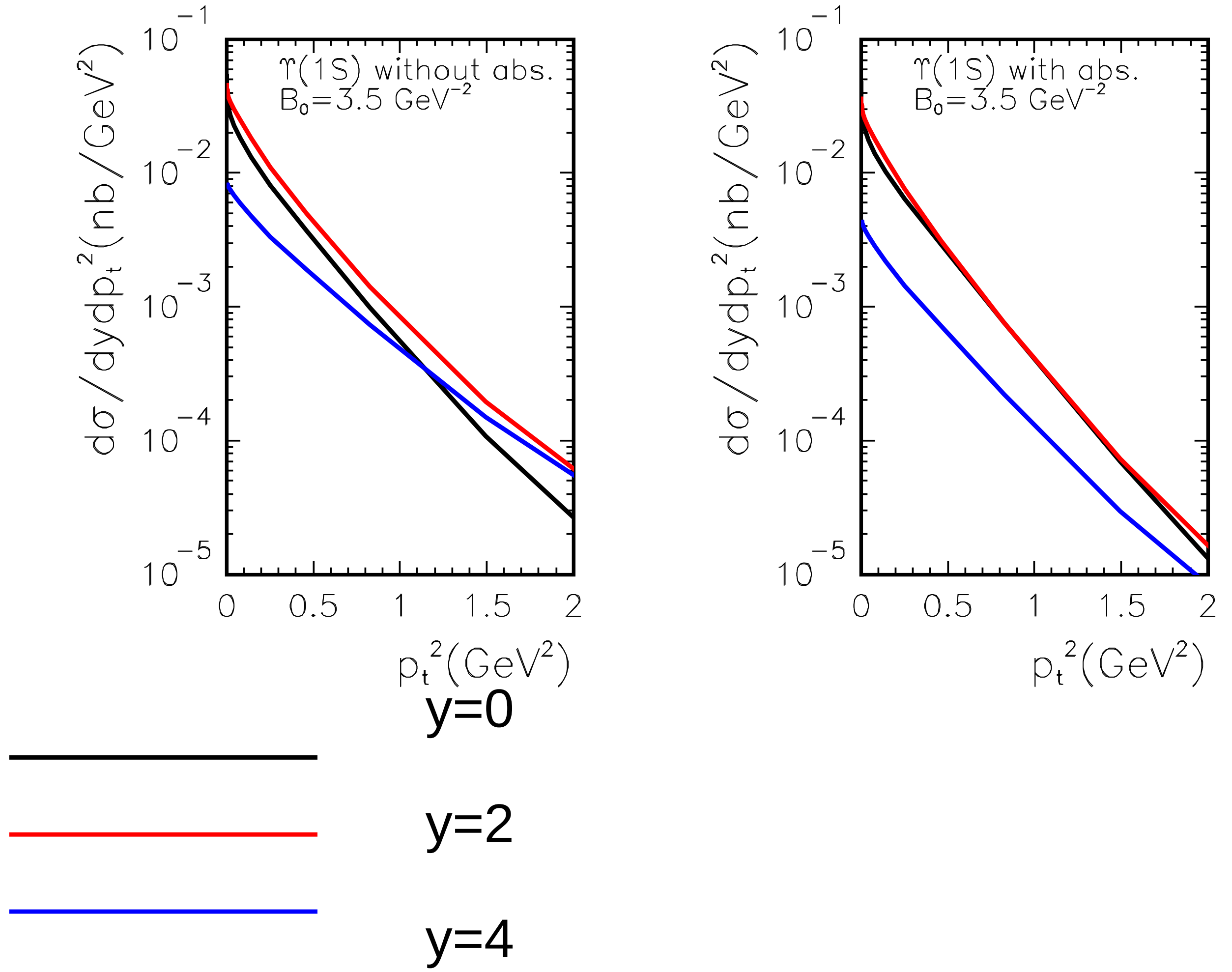

$d\sigma/dydp_t^2$ as a function of p_t^2 for Υ(2S)

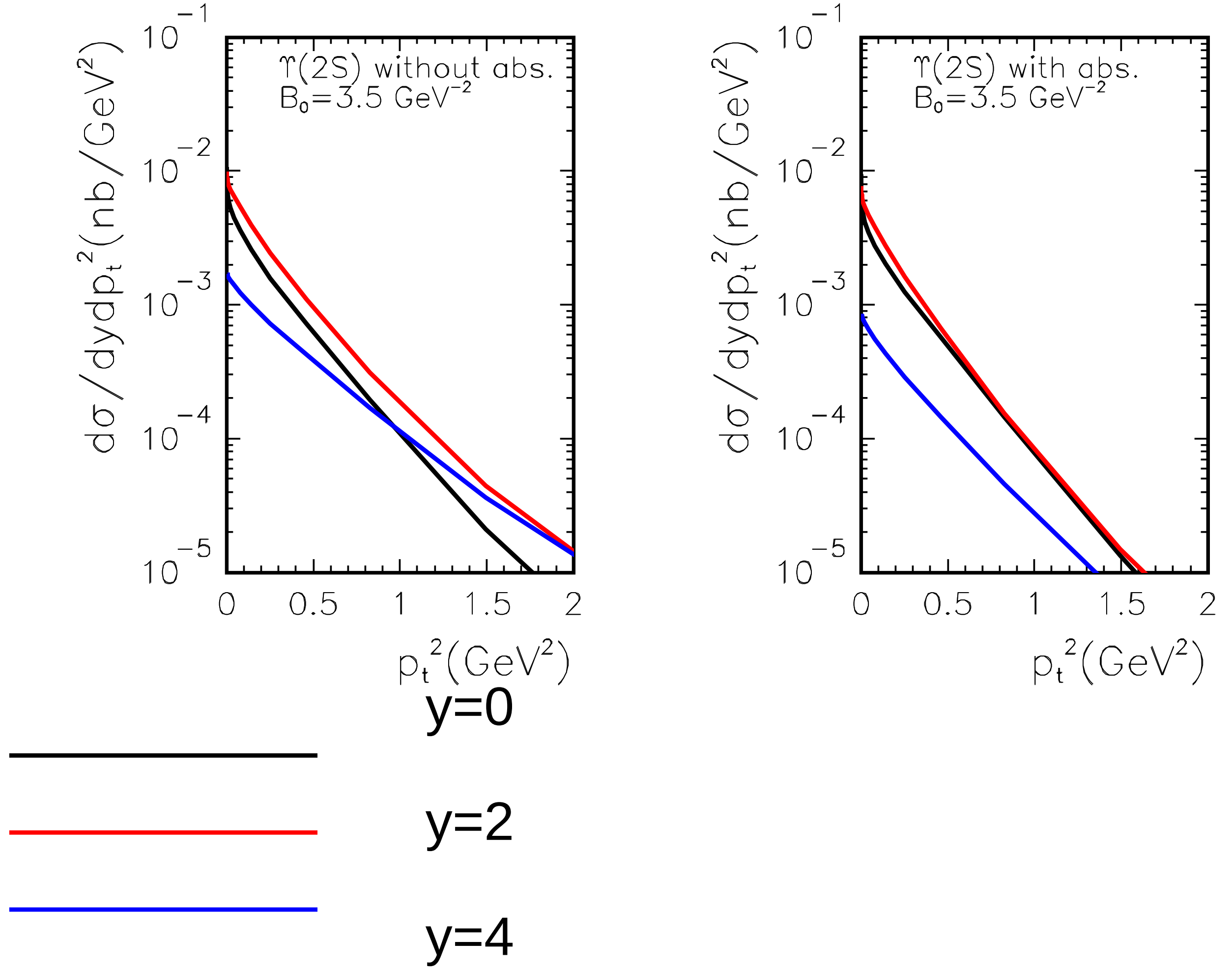

Absorption effects

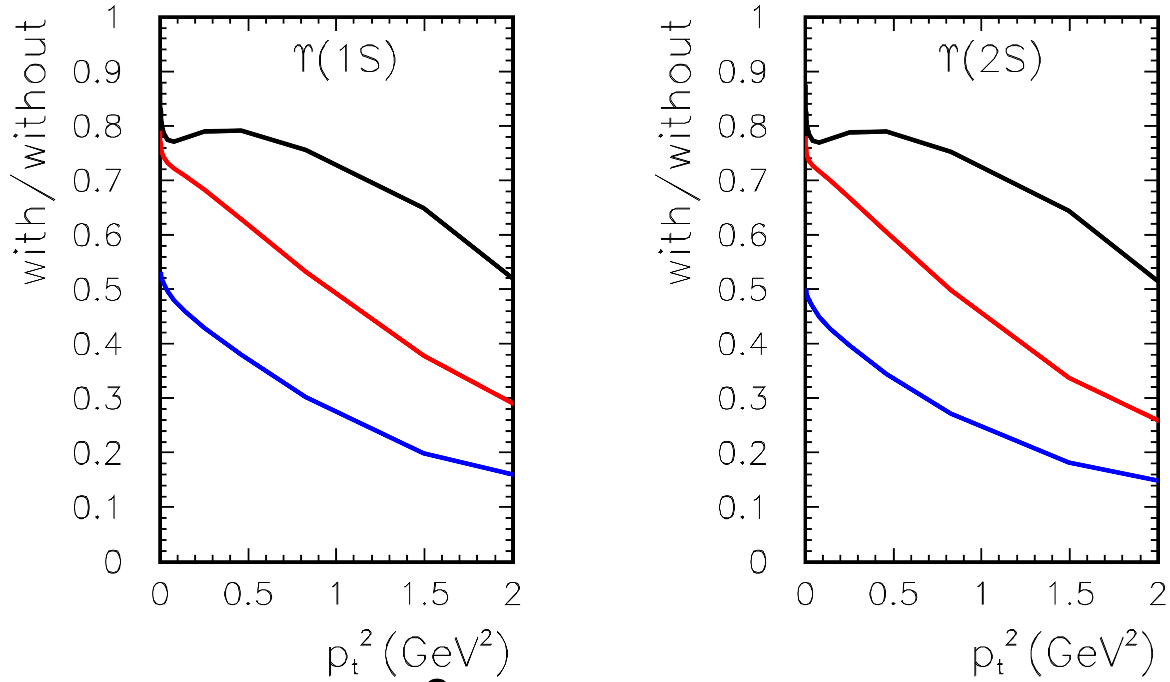

y=0

y=2

y=4

The bigger rapidity $\longrightarrow$ the bigger absorption effect

$d\sigma/dy$ - $J/\Psi, \Psi'$, Υ(1S) and Υ(2S) for Tevatron ar

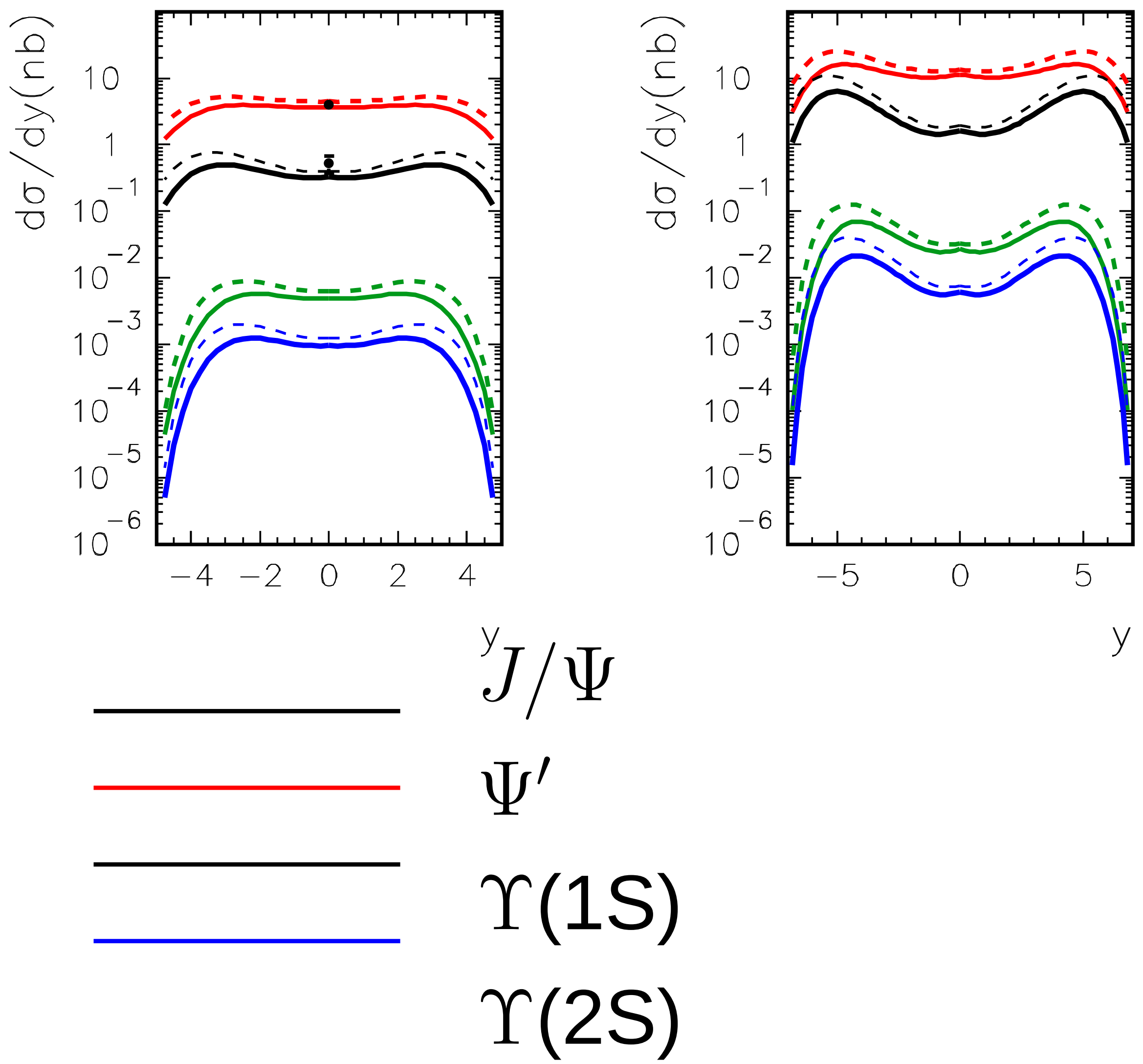

Summary of the Υ part

- The results for γp $\longrightarrow \Upsilon$ (1S) p production depend on the model of the wave function
- We have compared our results with a recent HERA data. Our results are somewhat lower than the HERA data but strong dependence on model details
- We have made predictions for $p\bar{p} \longrightarrow p\bar{p}\ \Upsilon$ for the FNL Tevatron (and LHC)
- Absorptive corrections have been included. They depend on p_t (Υ)

Exclusive $\pi^+\pi^-$ production in proton-proton collisions

P. Lebiedowicz + A.S.

High-energy mechanisms

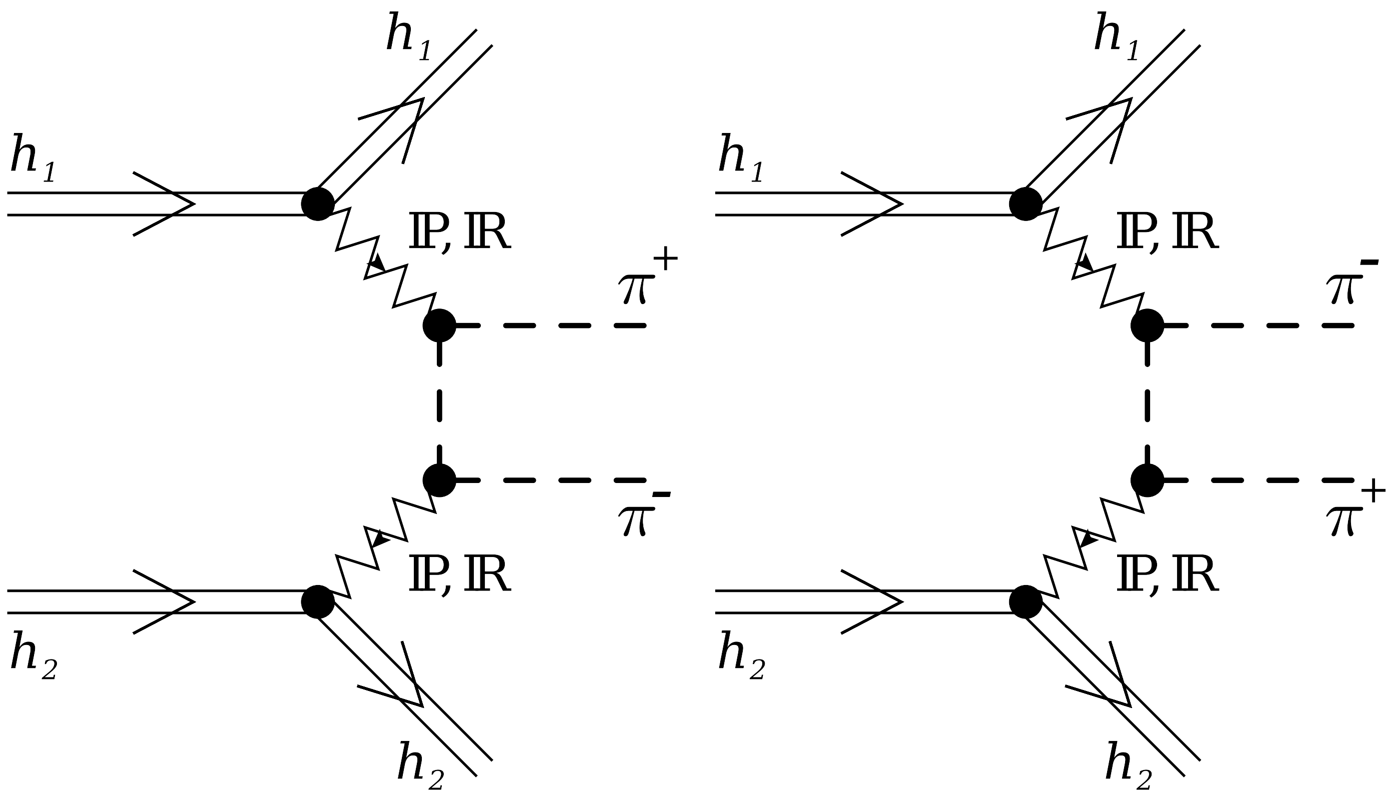

Pumplin model with Donnachie-Landshoff πN parameters and with exact four-body kinematics

Amplitude for $pp \to pp\pi^+\pi^-$

$$
\begin{aligned}
\mathcal{M}^{pp\to pp\pi\pi} \quad &= \quad M_{13}(t_1, s_{13})\; F(t_a)\, \frac{1}{t_a - m_\pi^2}\, F(t_a)\; M_{24}(t_2, s_{24}) \\
&+ \quad M_{14}(t_1, s_{14})\; F(t_b)\, \frac{1}{t_b - m_\pi^2}\, F(t_b)\; M_{23}(t_2, s_{13})\ ,
\end{aligned}
$$

where M_{ik} denotes "interaction" between nucleon and one of the two pions.

$$
\begin{aligned}
M_{13} &= i s_{13} \left(C_R^{13} \left(\frac{s_{13}}{s_0}\right)^{\alpha_R - 1} e^{\frac{B_{\pi N}}{2} t_1} + C_P \left(\frac{s_{13}}{s_0}\right)^{\alpha_P - 1} e^{\frac{B_{\pi N}}{2} t_1} \right) \\
M_{14} &= i s_{14} \left(C_R^{14} \left(\frac{s_{14}}{s_0}\right)^{\alpha_R - 1} e^{\frac{B_{\pi N}}{2} t_1} + C_P \left(\frac{s_{14}}{s_0}\right)^{\alpha_P - 1} e^{\frac{B_{\pi N}}{2} t_1} \right) \\
M_{24} &= i s_{24} \left(C_R^{24} \left(\frac{s_{24}}{s_0}\right)^{\alpha_R - 1} e^{\frac{B_{\pi N}}{2} t_2} + C_P \left(\frac{s_{24}}{s_0}\right)^{\alpha_P - 1} e^{\frac{B_{\pi N}}{2} t_2} \right) \\
M_{23} &= i s_{23} \left(C_R^{23} \left(\frac{s_{23}}{s_0}\right)^{\alpha_R - 1} e^{\frac{B_{\pi N}}{2} t_2} + C_P \left(\frac{s_{23}}{s_0}\right)^{\alpha_P - 1} e^{\frac{B_{\pi N}}{2} t_2} \right) \qquad (33)
\end{aligned}
$$

Elastic $\pi^+ p$ and $\pi^- p$ scattering

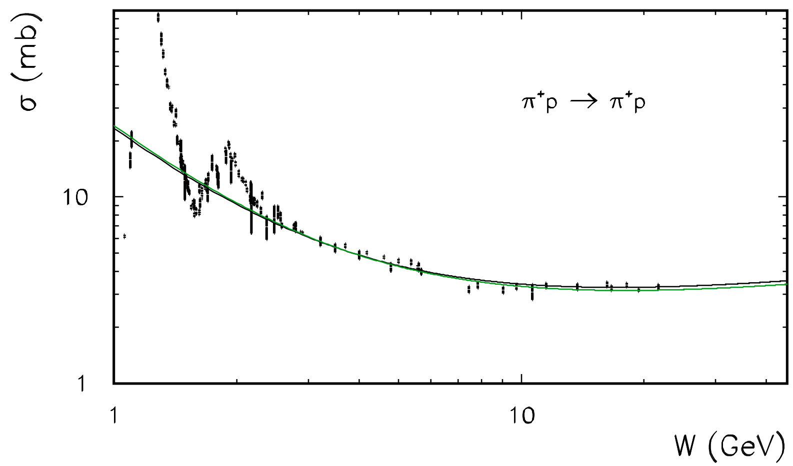

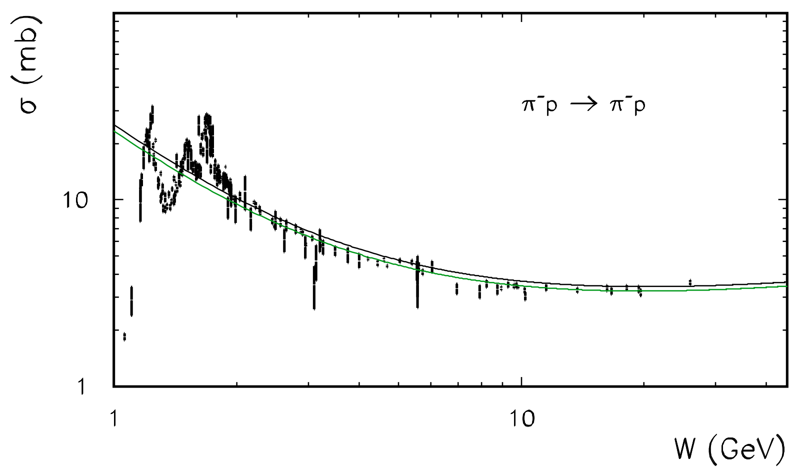

Amplitude for $pp \to pp\pi^+\pi^-$

$F(t_a)$ and $F(t_b)$ form factors "correct" for off-shellness of the intermediate pion (kaon).

$$F(t) = \exp \frac{(t - m_\pi^2)}{\Lambda^2} \; , \tag{34}$$

i.e. normalized to unity on the pion-mass-shell.
To exclude resonance regions we "correct" parametrization (33) by multiplying:

$$f_{cont}^{\pi N}(W_{ik}) = \frac{x}{1+x} \; , \tag{35}$$

where $x = \exp\left(\frac{W - W_0}{a}\right)$. The parameter W_0 gives the position of the cut and a describes how sharp is the cut off.

Correlation in rapidity of both pions

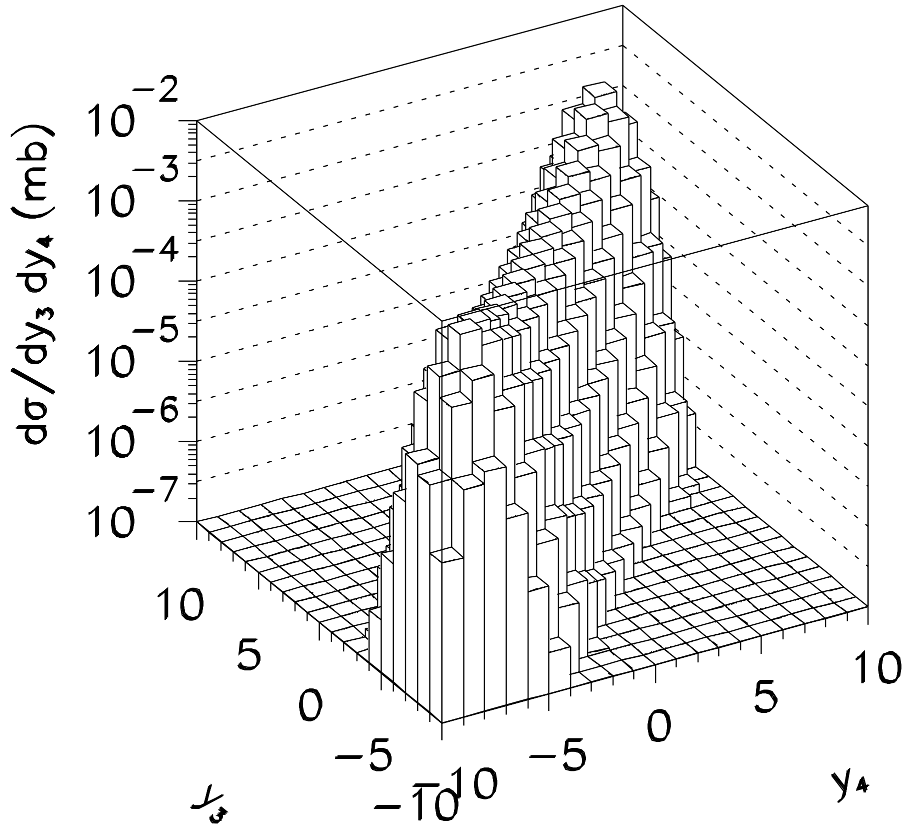

Rapidity distribution of final particles

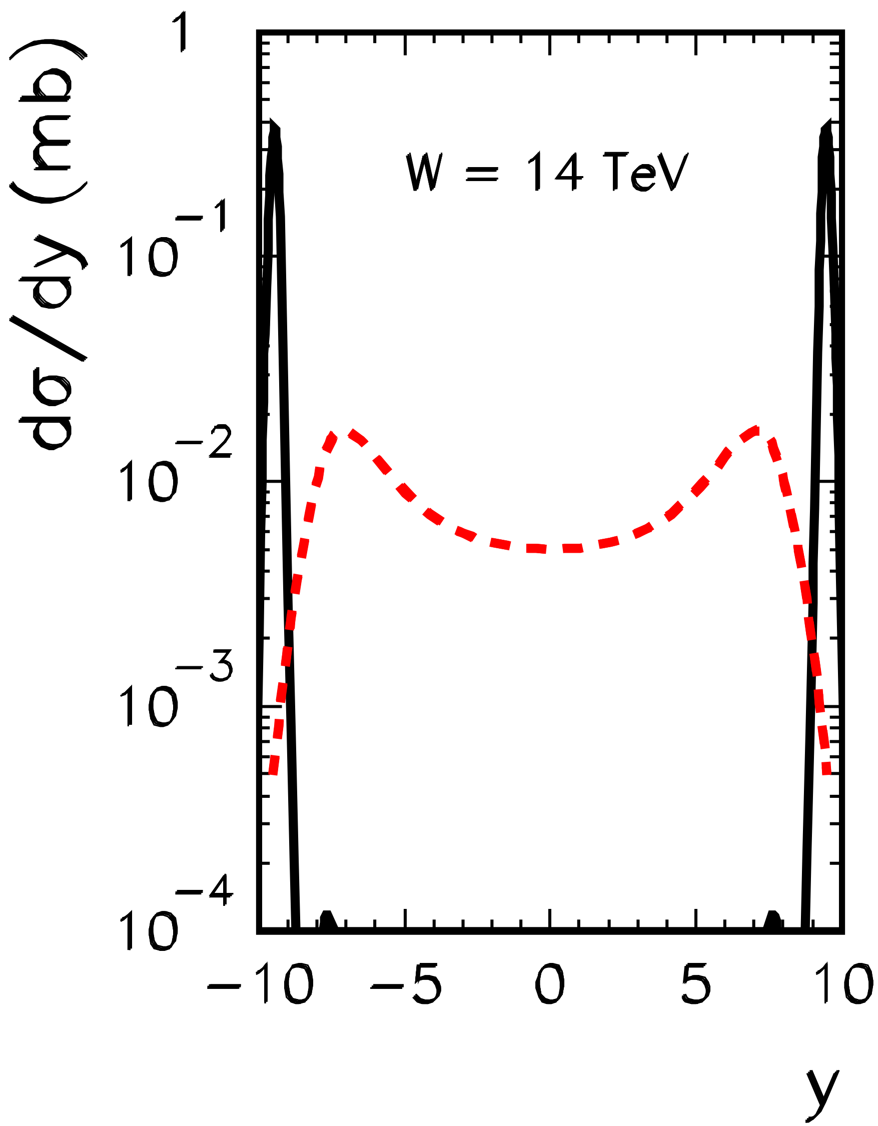

Feynman variable distribution of final particles

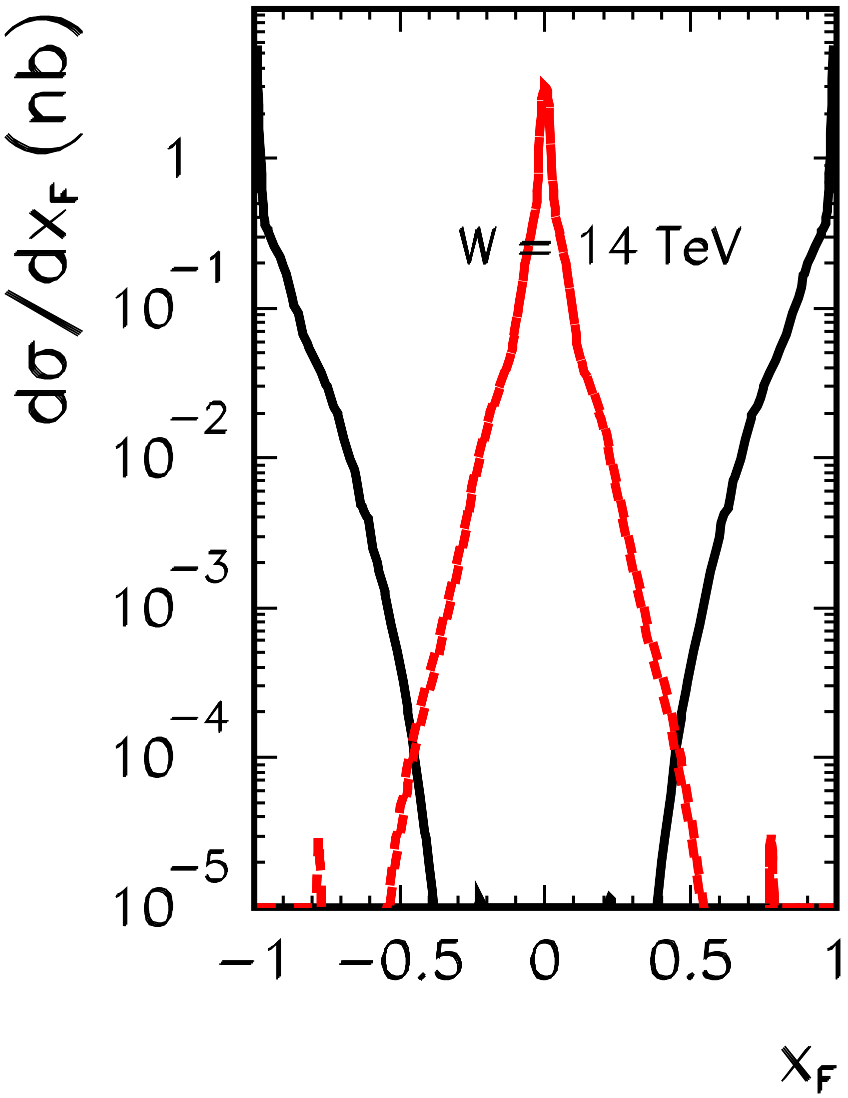

Transverse momentum distribution of final par

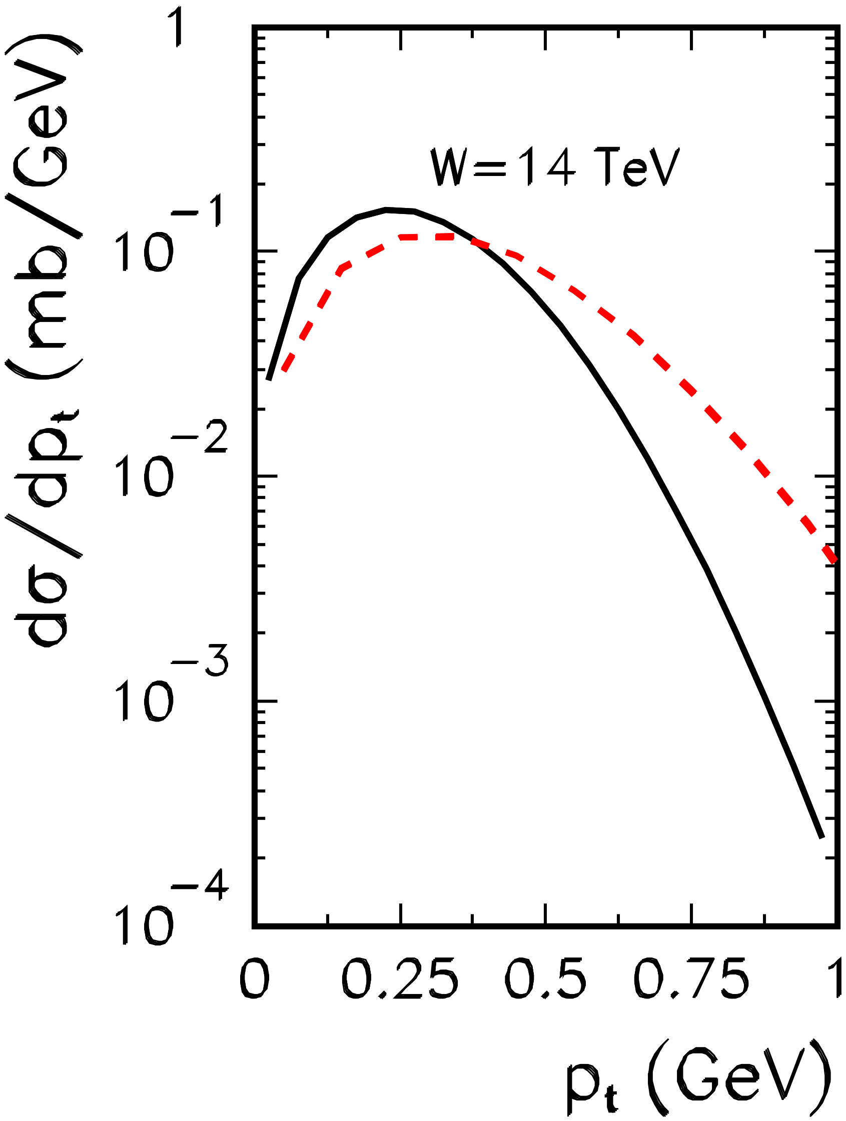

Azimuthal correlation between π^+ and π^-

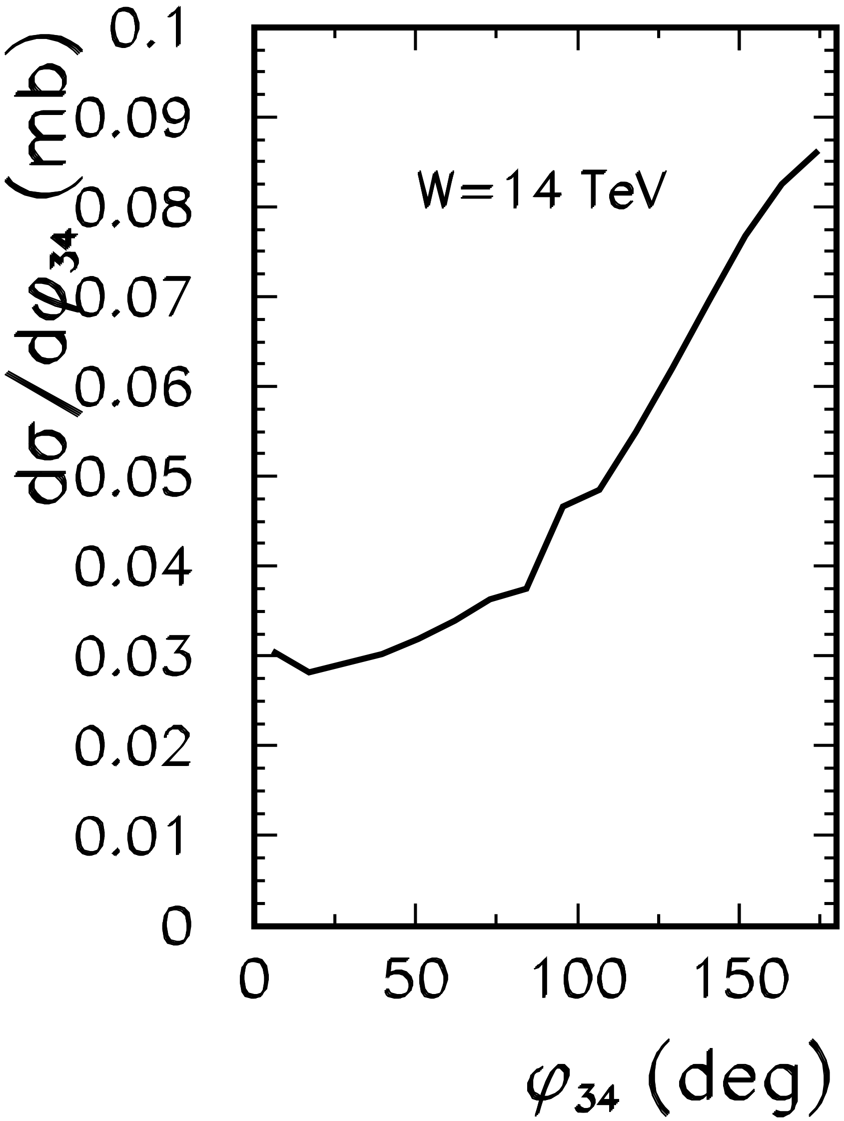

Distribution of pions

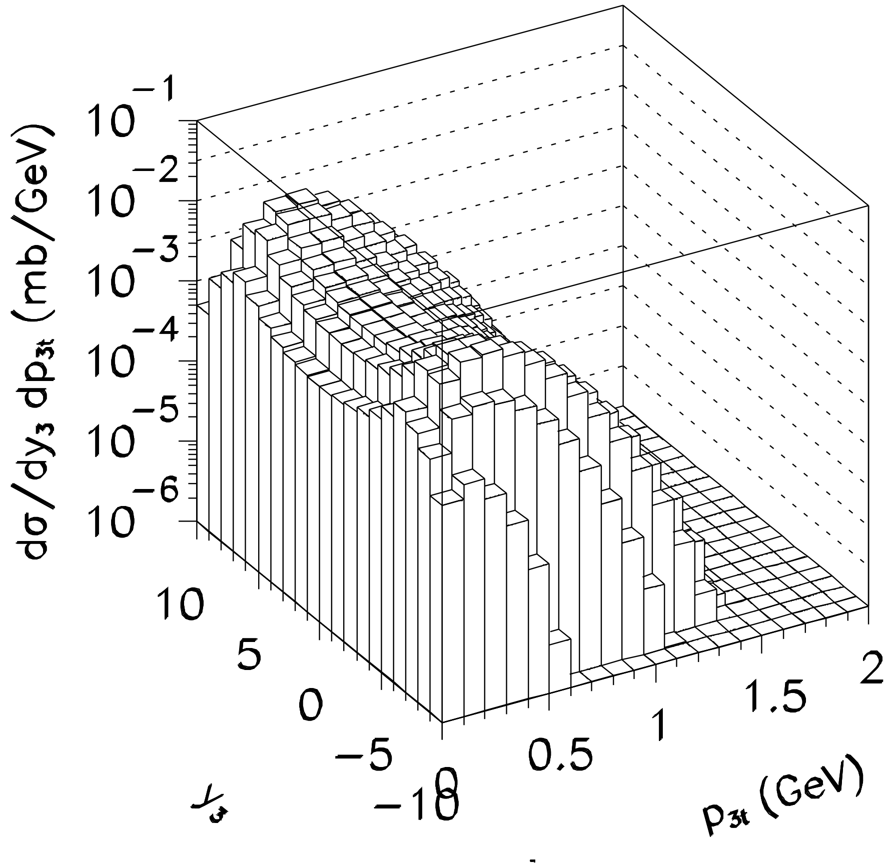

Correlations in transverse momenta of pions

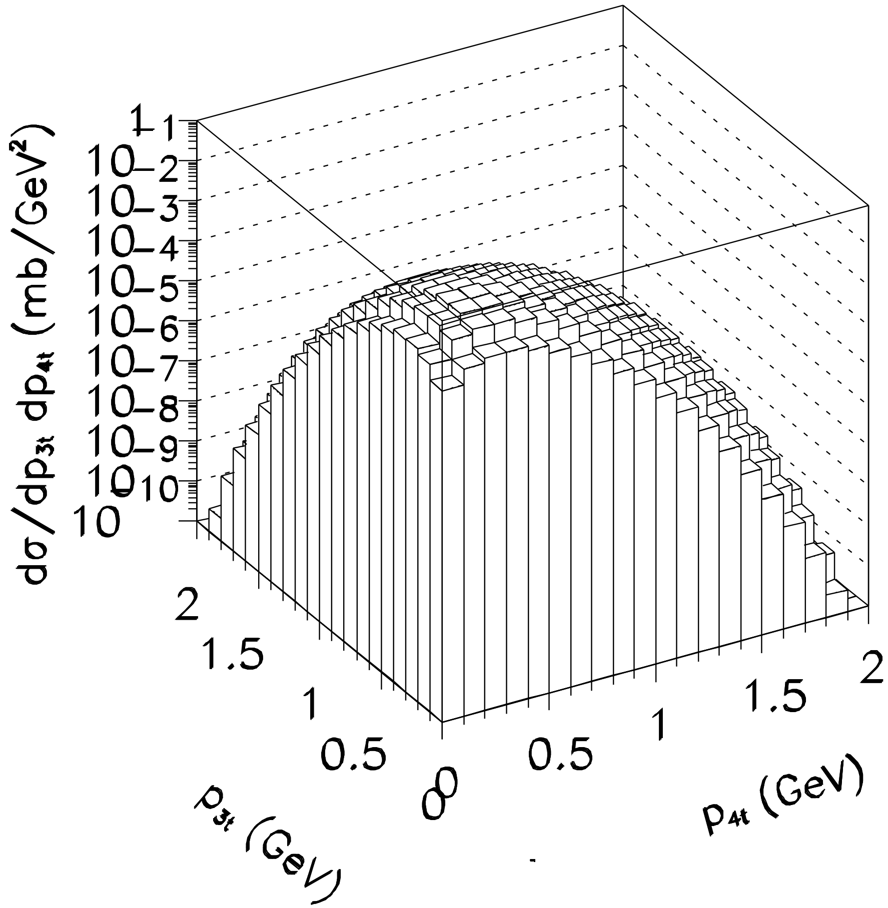

Summary of two-pion part

- Large cross sections ($\sim$ 50 - 100 μb)
- Strong interference effects at "low" energies:
  (a) two crossed channels
  (b) pomeron and reggeon exchanges
- At high energy both pions emitted in the same hemisphere
- Nucleons almost not correlated, pions correlated in relative azimuthal angle
- Is a measurement possible ?

Exclusive $AA \to AA\rho^0\rho^0$ at ultrarelativistic collisions

M. Klusek, W. Schafer and A.S

$AA \rightarrow AA\rho^0\rho^0$

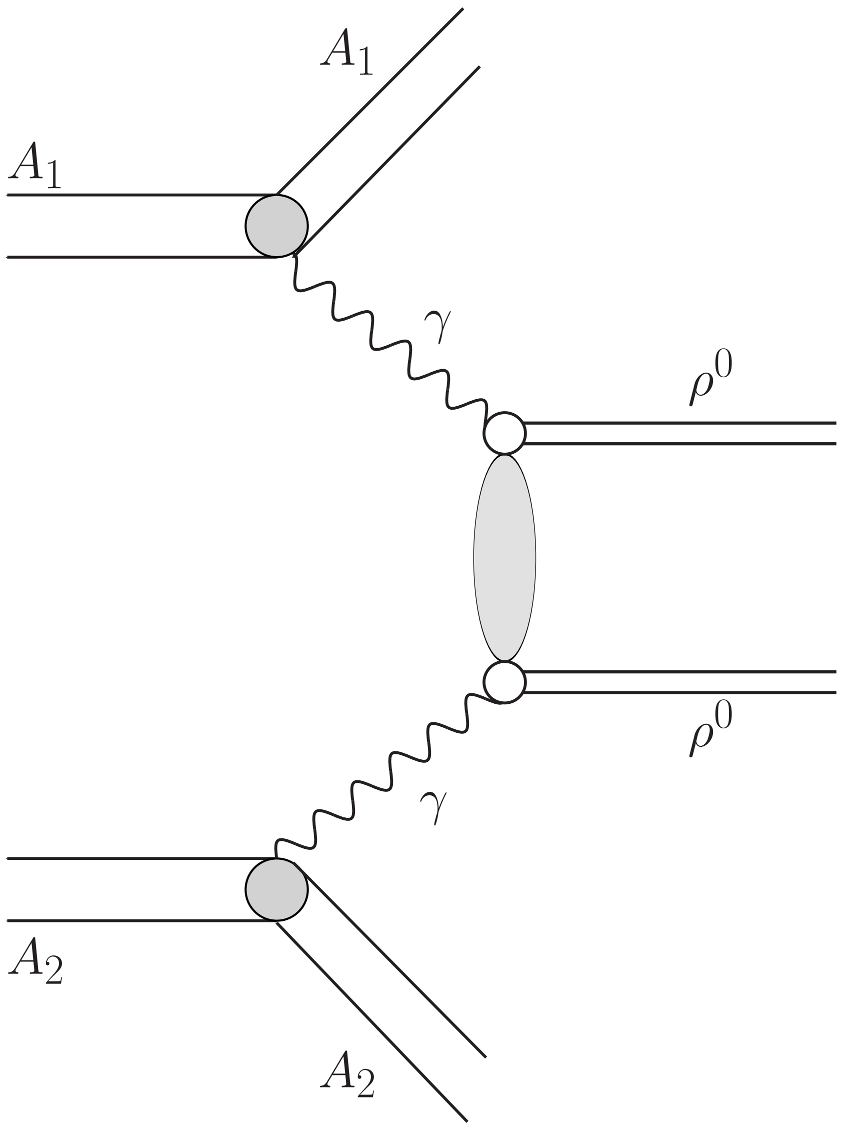

Equivalent photon approximation, part 1

For point-like charges:

$$\sigma\left(AA \to A(\rho^0\rho^0)A\right) = \int d\omega_1 d\omega_2 \frac{n(\omega_1)}{\omega_1}\frac{n(\omega_2)}{\omega_2}\hat{\sigma}\left(\gamma\gamma \to \rho^0\rho^0\right) . \tag{36}$$

$$\sigma\left(AA \to A(\rho^0\rho^0)A\right) = \int dW\,dY \frac{W}{2}\frac{n(\omega_1)}{\omega_1}\frac{n(\omega_2)}{\omega_2}\hat{\sigma}\left(\gamma\gamma \to \rho^0\rho^0\right) , \tag{37}$$

where $\omega_1 = \frac{W}{2}e^{Y}$ and $\omega_2 = \frac{W}{2}e^{-Y}$.

Collision geometry

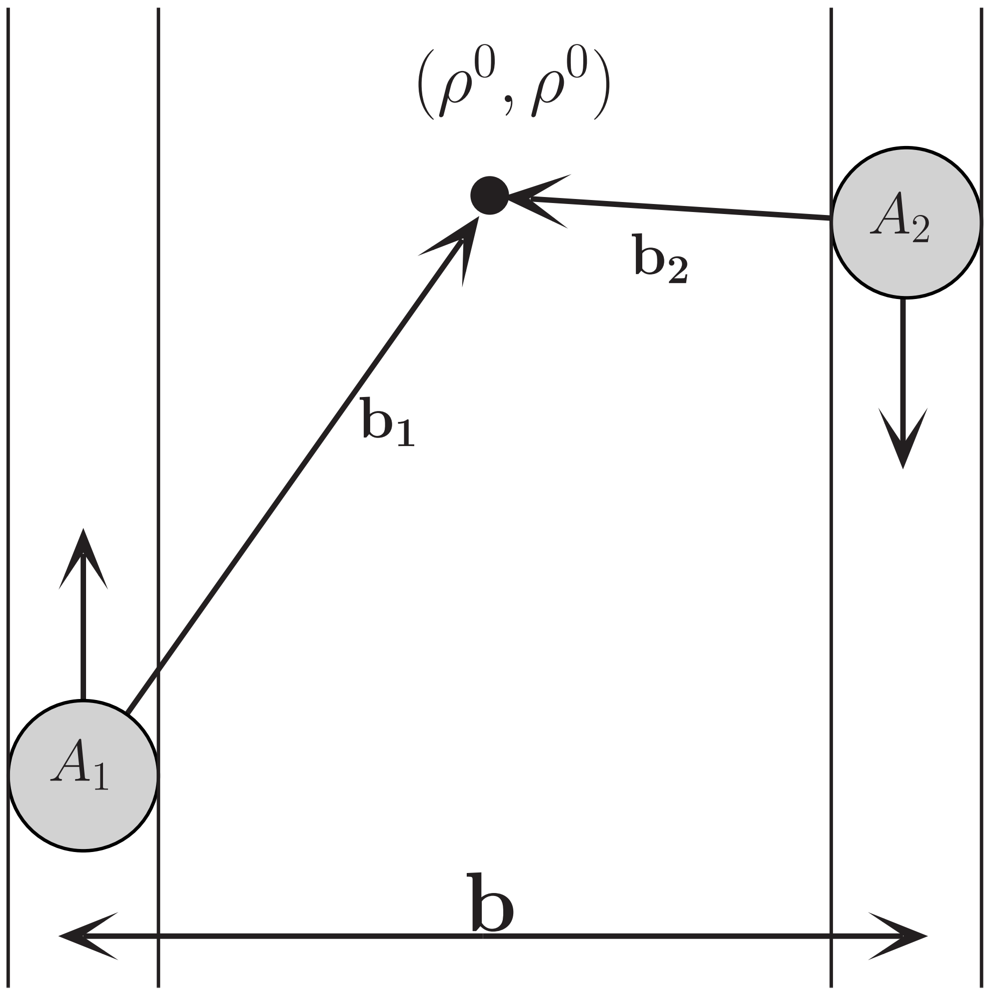

Equivalent photon approximation, part 2

The simple EPA formula has to be generalized to include process geometry (absorption)

$$\sigma\left(AA \to A(\rho^0\rho^0)A\right) = \int d^2b_1 d\omega_1 d^2b_2 d\omega_2 N(\omega_1, b_1) N(\omega_2, b_2)\, \theta\left(|\vec{b}_1 - \vec{b}_2| - R_{12}\right) \hat{\sigma}\left(\gamma\gamma \to \rho^0\rho^0\right. \tag{38}$$

θ function excludes those cases when nucler collisions, take place ($R_{12} = R_1 + R_2$).

$$N(w,b) = \frac{Z^2\alpha}{\pi^2}\Phi(x,b)\ , \tag{39}$$

where

$$\Phi(x,b) = |\int_0^\infty du\ u^2 J_1(u)\ \frac{F(-(x^2+u^2)/b^2)}{x^2+u^2}|^2 \tag{40}$$

in the literature: $F(q)$ from simplified parametrizations
here: Fourier transform of charge density $\rho(r)$

Low-energy $\gamma\gamma \to \rho^0\rho^0$

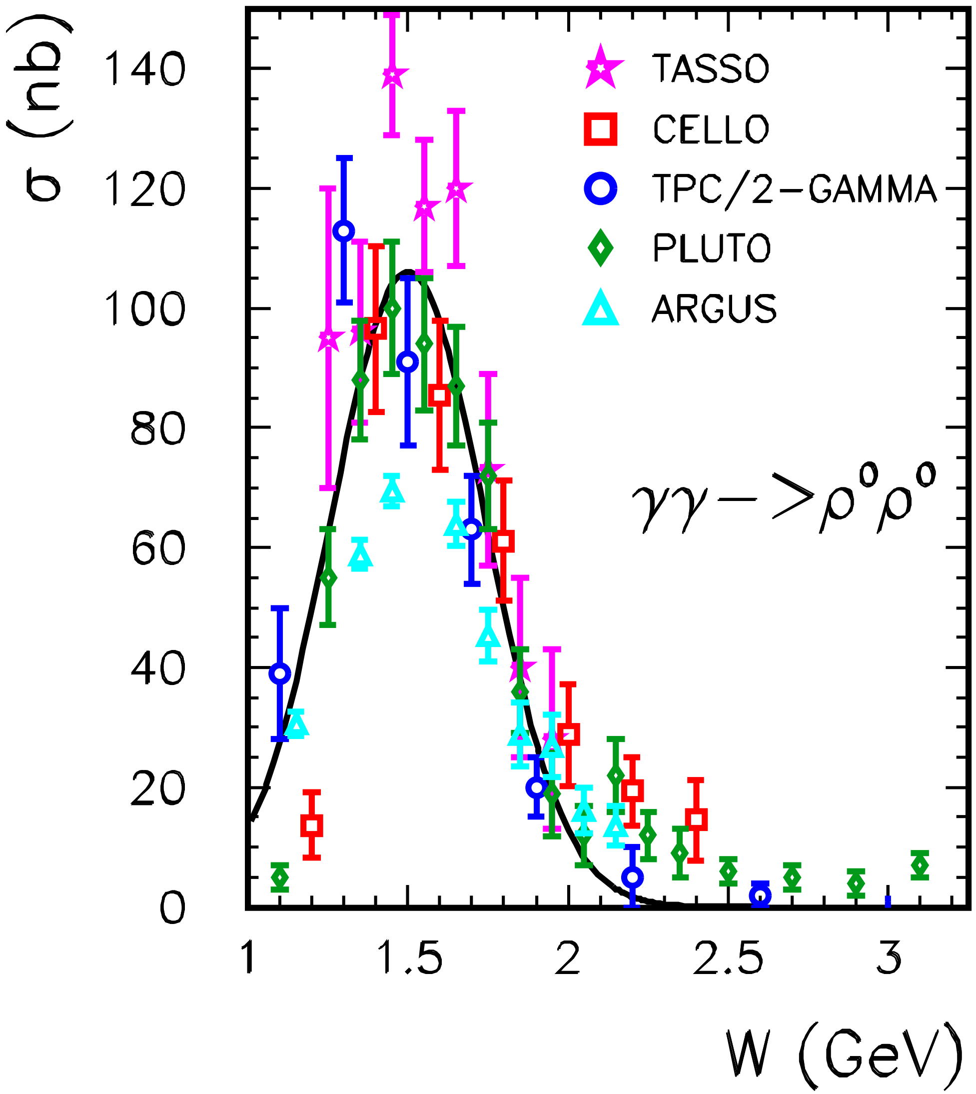

High-energy $\gamma\gamma \to \rho^0 \rho^0$

In the VDM approach|:

$$\mathcal{M}_{\gamma\gamma \to \rho^0\rho^0}(\hat{s}, \hat{t}; q_1, q_2) = C_{\gamma \to \rho^0} C_{\gamma \to \rho^0} \mathcal{M}_{\rho^{0*}\rho^{0*} \to \rho^0\rho^0}(\hat{s}, \hat{t}; q_1, q_2) \,. \tag{41}$$

Above $C_{\gamma \to \rho^0} = \sqrt{f_\rho^2}$ and we use $f_\rho^2 = \frac{\alpha_{em}^2}{2.54}$.
For $W_{\gamma\gamma} >$ 2-3 GeV the amplitude in the Regge form:

$$\mathcal{M}_{\rho^{0*}\rho^{0*} \to \rho^0\rho^0}(\hat{s}, \hat{t}) = \hat{s} \left(\eta_{IP}(\hat{s}, \hat{t})\, C_{IP} \left(\frac{\hat{s}}{s_0} \right)^{\alpha_{IP}(\hat{t})-1} + \eta_{IR}(\hat{s}, \hat{t})\, C_{IR} \left(\frac{\hat{s}}{s_0} \right)^{\alpha_{IR}(\hat{t})-1} \right) \cdot F(\hat{t}; q_1^2 \tag{42}$$

Form factors parametrized in the factorized form:

$$F(\hat{t}; q^2) = \exp\left(\frac{B\hat{t}}{4} \right) \cdot \exp\left(\frac{q^2 - m_\rho^2}{2\Lambda^2} \right) \,. \tag{43}$$

$B \sim 4$ GeV^{-2}, $\Lambda \sim 1$ GeV.
α_{IP}, α_{IR} from the Donnachie-Landshoff fit to the total NN and πN. C_{IP} and C_{IR} from Regge factorization and assuming $\sigma(\rho^0\rho^0 \to \rho^0\rho^0) = \sigma(\pi^0\pi^0 \to \pi^0\pi^0)$.

$$\frac{d\sigma_{\gamma\gamma \to \rho^0\rho^0}}{d\hat{t}} = \frac{1}{16\pi\hat{s}^2} |\mathcal{M}_{\gamma\gamma \to \rho^0\rho^0}|^2 \,. \tag{44}$$

Charge form factor of ^{197}Au

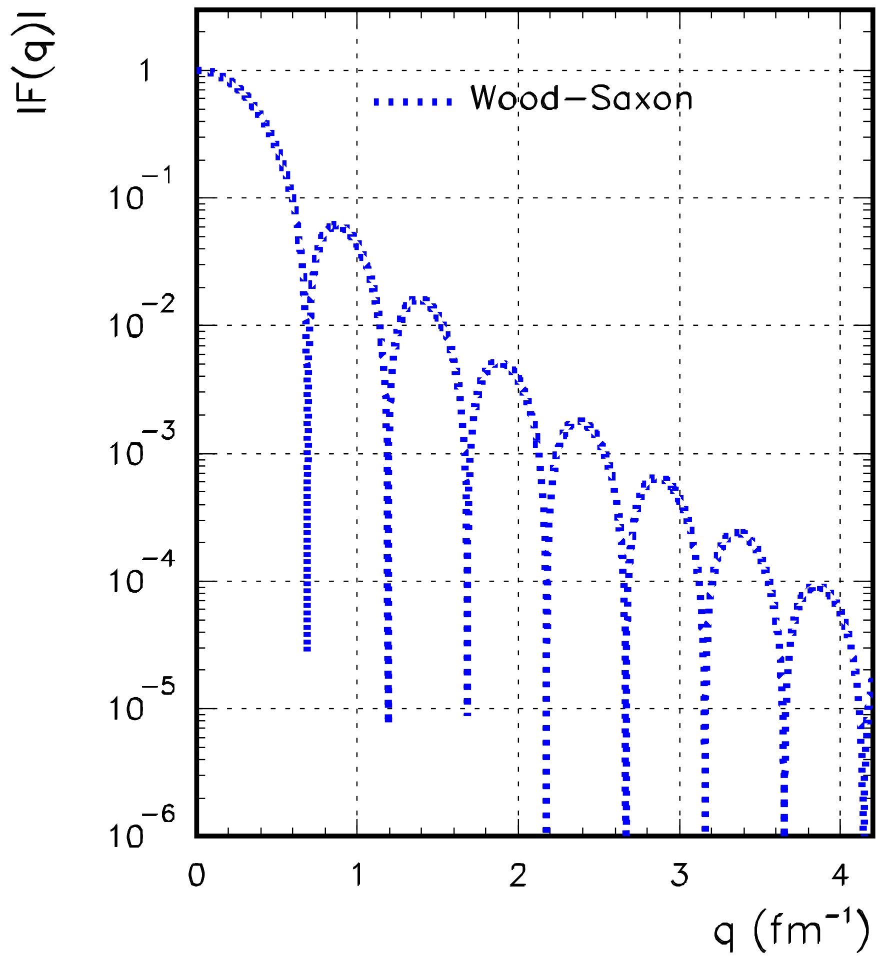

Impact factor distribution

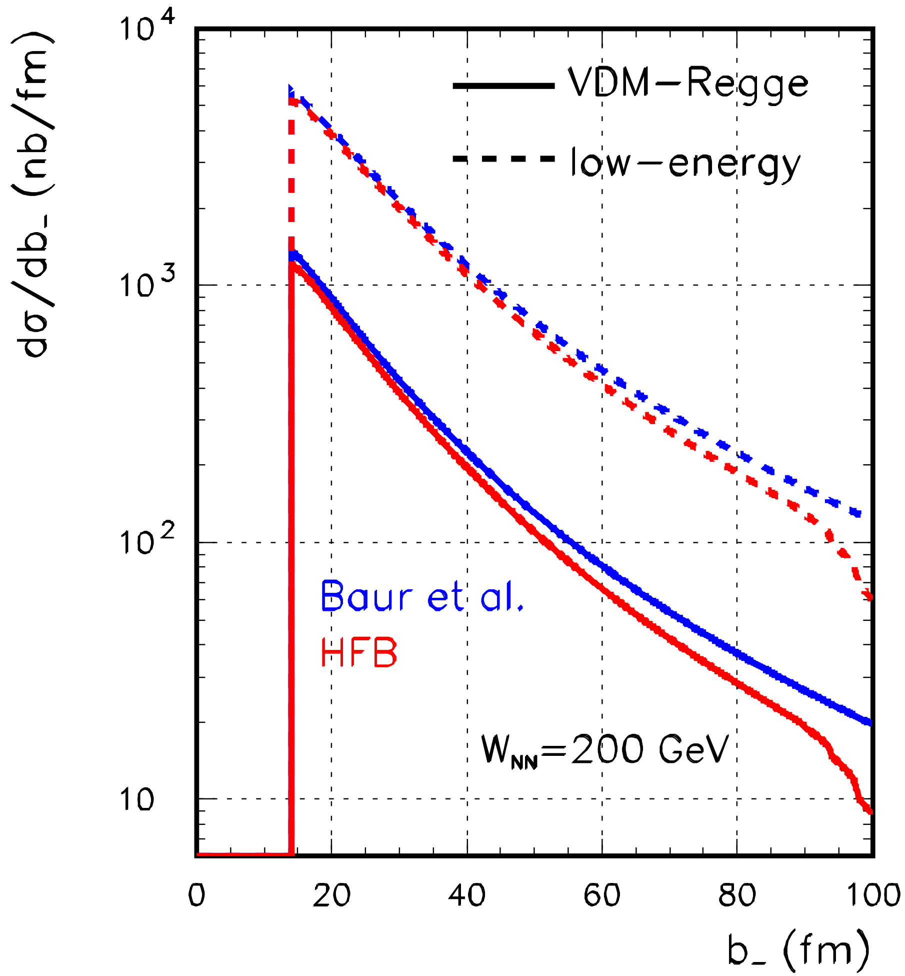

$W_{\gamma,\gamma}$ distribution

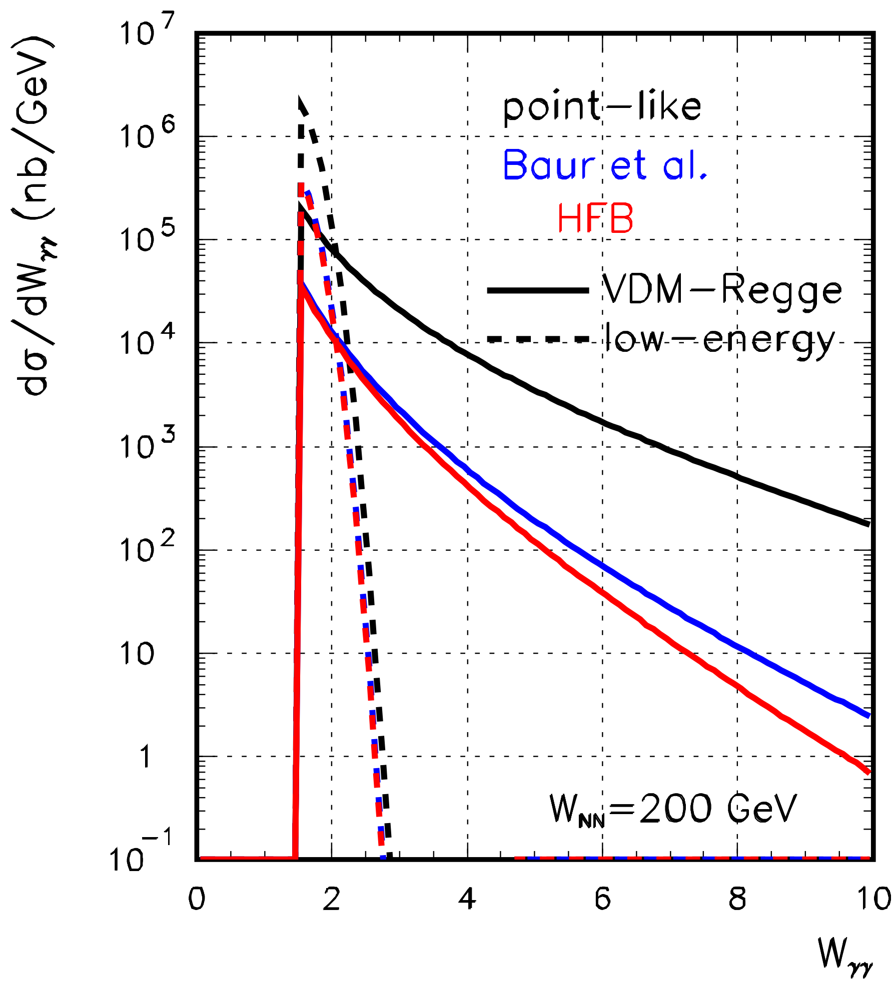

Distribution in rapidity of the $\rho^0\rho^0$ pair

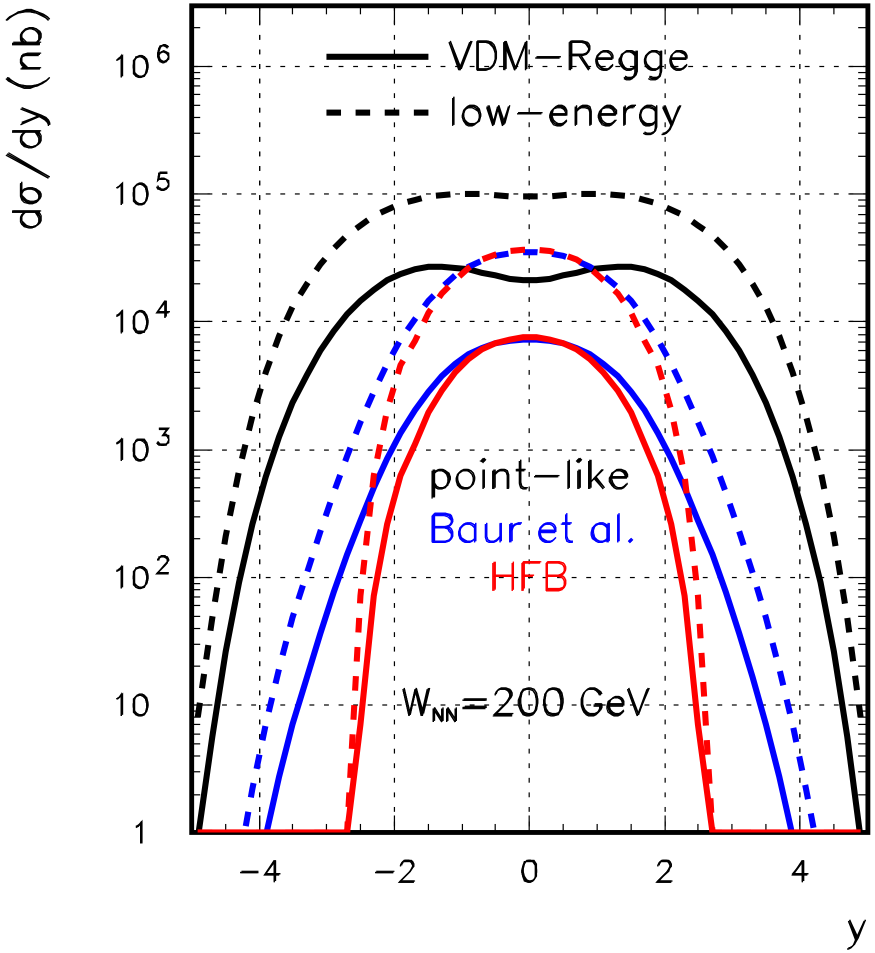

Summary of the $AA \to AA\rho^0\rho^0$ part

- Large cross sections of several μb
- Dominance of low-energy $\gamma\gamma \to \rho^0\rho^0$ scattering. Much higher cross section than in previous evaluation.
- Use of realistic charge densities very important. It lowers the cross section.
- Is a measurement possible ?